New generic coupling adapters for ice sheet and subglacial hydrology models (ISSM-preCICE Adapter 0.4, CUAS-MPI 0.1)

Daniel Abele[1,2,3], Thomas Kleiner[2], Yannic Fischler[4], Benjamin Uekermann[5], Gerasimos Chourdakis[5], Mathieu Morlighem[6], Achim Basermann[1], Christian Bischof[4], Hans-Joachim Bungartz[3], and Angelika Humbert[2,7]

[1]German Aerospace Center, Institute of Software Technology, Oberpfaffenhofen/Cologne, Germany
[2]Alfred-Wegener-Institut, Helmholtz-Zentrum für Polar- und Meeresforschung, Bremerhaven, Germany
[3]School of Computation, Information, and Technology, Technical University of Munich, Germany
[4]Department of Computer Science, Technical University Darmstadt, Germany
[5]Institute for Parallel and Distributed Systems, University of Stuttgart, Germany
[6]Department of Earth Sciences, Dartmouth College, Hanover, NH, USA
[7]Faculty of Geosciences, University of Bremen, Germany

Correspondence: Daniel Abele (daniel.abele@dlr.de)

Abstract. Adequate ~~earth~~ Earth system simulations require interactions between the atmosphere, the ocean, and the ice sheets. To this end, numerical solvers that compute the evolution of the different ~~earth~~ Earth system components are coupled. There are frameworks and libraries for coupling that handle the complex tasks of coordinating solver execution, communicating between processes, and mapping between different meshes. This allows solvers to be developed independently without compromises on numerical methods or technology. Code reuse is improved, both over large, monolithic software systems that reimplement each coupled model as well as over ad-hoc coupling scripts.

In this work, we use the ~~preCICE~~ preCICE coupling library to couple the Ice-sheet and Sea-level System Model (~~ISSM~~ISSM) with the subglacial hydrology model ~~CUAS-MPI~~CUAS-MPI. An adapter for each model is required to pass meshes and coupled variables between the model and ~~preCICE~~preCICE. We focus mainly on the technical aspects (design, development, and use of the adapters, choice of coupling library, and large-scale performance analysis), using a synthetic setup to verify functionality and correctness.

The adapters we developed are generic ~~,~~ and reusable for use cases other than ice-hydrology coupling. Computational performance for the coupled system is measured on a high-performance computing cluster. We find that coupling with ~~preCICE~~ preCICE has low computational overhead and does not negatively impact scaling. A comparison between unidirectional and bidirectional coupling for the synthetic ice sheet shows that the coupling captures the anticipated feedback mechanisms between the two systems. The coupled simulations are numerically stable, despite the nonlinearities in the physical system. The generic coupling library ~~preCICE~~ preCICE is well suited for our use case and has advantages as well as disadvantages over ~~earth system model specific~~ Earth System Model-specific libraries.

The new framework and code ~~enables~~ enable studies of the subglacial ~~hydrology~~ hydrological systems of ice sheets, as well as coupling ~~ISSM or CUAS-MPI~~ ISSM or CUAS-MPI with other codes, such as in global ~~earth system models~~ Earth System Models or process models.

1 Introduction

Ice sheet dynamics is a gravity-driven, lubricated flow, forced by changes at its boundaries, such as the ice-atmosphere interface, the ice-ocean interface and the conditions at the ice base. Beneath the ice sheet, a subglacial hydrological system exists that is formed fed by basal melting due to heat flux from the lithosphere and frictional heatheating. This hydrological system affects the ice sheet through changes in water pressure, while the ice sheet influences the subglacial system through changes in basal melt rates and ice sheet thickness. While the hydrological system evolves on long time scales in the center of ice sheets, at the margins, particularly in Greenland during the melt season, the evolution is accelerated considerably. Both observations (Ing et al., 2024) and modeling (de Fleurian et al., 2022) have shown the high complexity of the feedback between hydrology and ice sheet. Therefore, coupled simulations are required to study the evolution of both systems and their effect on each other. As both systems include non-linear processes, special care is required when simplifying the interactions of the system to a uniphysics problem, as also suggested by (Keyes et al., 2013)Keyes et al. (2013). This work presents a framework for simulating interactions as a multiphysics problem and applies it to an artificial setup and to Greenland.

The Ice-Sheet and Sea-level System Model (ISSM, Larour et al., 2012) (ISSM, Larour et al., 2012) is a feature-rich ice sheet model. Among its capabilities, it provides a selection of subglacial hydrology models, including the Subglacial Hydrology and Kinetic, Transient Interactions model (SHAKTI, Sommers et al., 2018), the Glacier Drainage System (GlaDS, Werder et al., 2013), and the Double-Continuum model (DoCo, de Fleurian et al., 2016). These models are fully integrated into ISSMISSM, using the same mesh and finite-element solvers. GLaDS GLaDS is also included in the ice sheet model Elmer/Ice (Gagliardini et al., 2013). Other ice sheet modelslike PISM (Khrulev et al., 2025), like PISM (Khrulev et al., 2025), also have their own hydrology models. While monolithic software development can be easier (e.g., only one build process , sharing the same a single build process and shared data structures), it also comes with disadvantageshas disadvantages, including increased complexity and reduced reusability.

In this paper, we present a different, partitioned approach. Fischler et al. (2023) recently published CUAS-MPI CUAS-MPI (subsequently referred to as CUASCUAS), a stand-alone subglacial hydrology model. ISSM and CUAS ISSM and CUAS rely on different spatial and temporal discretizations, so CUAS CUAS cannot be directly integrated into ISSM. We ISSM. To couple the two models, we use an external independent coupling library, namely the general coupling library preCICE (Chourdakis et al., 2022). To this end, we general-purpose coupling library preCICE (Chourdakis et al., 2022). We developed adapters for both models that link them to preCICEpreCICE. This approach has a number of advantages over integrating CUAS directly into ISSMseveral advantages over directly integrating CUAS into ISSM. The models can be developed independently and make their own choices regarding discretization and numerical methods. Moreover, coupling libraries, such as preCICEpreCICE, make the setup more configurable and extendable – for instance, towards by adding further components like an existing ocean circulation model or replacing existing components.

preCICE, as As a general-purpose coupling library, preCICE follows an application-agnostic coupling approach. This is in contrast to specialized earth system modeling Earth System Modeling (ESM) couplers, such as OASIS3-MCT (Craig et al., 2017)or , YAC (Hanke et al., 2016). , or ESMF (ESMF Core Team, 2026). While any of these couplers could have been used in

principle, using preCICE allows us to evaluate it in a context in which it has not been extensively tested yet. Specialized couplers offer coupling methods, particularly data mapping methods, which are optimized to handle 2D fields on spherical surface meshes and are, thus, well suited to model global effects on the whole ~~earth. preCICE~~Earth. preCICE, in contrast, treats meshes as clouds of scattered Cartesian points. ~~Hocks and Uekermann (2026) compares the general data mapping of preCICE to those of specialized couplers using an ESM mapping benchmarks and concludes that preCICE is competitive. While specifically the radial-basis-function interpolation performs well for the considered smooth test functions, preCICE still lacks specialized~~ A manuscript in review studies the viability of this approach for global models (Hocks and Uekermann, 2026). In addition, preCICE lacks conservative data mappings~~– a limitation that can, however, be overcome by bespoke pre- and postprocessing. The missing ESM specialization of preCICE~~ [1], among other specialized features. However, the missing specialization of preCICE is less important in non-global ESM scenarios, such as the setup of this paper, ~~or scenarios where more flexibility is needed such as adding further models.~~

~~The functionality of preCICE goes beyond communication and data mapping, as specialized ESM couplers typically offer. Implicit coupling schemes including quasi-Newton acceleration (Mehl et al., 2016) ,~~ and it also provides features such as implicit coupling schemes (Mehl et al., 2016) and time interpolation (Rodenberg and Uekermann, 2025) ~~, or multi-scale coupling (Desai et al., 2023) are all features that are relevant for ESM . Moreover,~~ that are not typically offered by ESM couplers and could provide benefits to some applications.

Beyond different feature sets, while specialization allows for more focused development, the generality of ~~preCICE activates a large user and develop community, which brings further potential soft benefits~~preCICE also brings the soft benefits of a potentially larger user and developer community: cross-domain knowledge transfer, ~~extensive user documentation, sustainability of the~~ more sustainable software development, and integration in widely used simulation software, ~~for example~~e.g. OpenFOAM (Chourdakis et al., 2023) and FEniCS (Rodenberg et al., 2021), that can be used to develop new models.

Sect. 2 of this manuscript covers the software packages that are involved. First, we describe the coupling library ~~preCICE~~ preCICE and the existing solvers[2] ~~ISSM and CUAS~~ISSM and CUAS. Then, we present the newly developed adapters. In Sect. 3, we show the setup and results of a few basic experiments we performed to test the coupling and the computational performance. In Sect. 4, we discuss our findings and plans for future development.

2 Software

In the following, we describe all the software components necessary for the coupling of ~~ISSM and CUAS~~ISSM and CUAS. Fig. 1 shows an overview of the coupling setup. We provide brief summaries of the three existing codes, with a focus on the technical details relevant to coupling: the ~~preCICE~~ preCICE coupling library, the ice-sheet model ~~ISSM~~ISSM, and the subglacial hydrology model ~~CUAS~~CUAS. The newly developed ~~preCICE adapters for ISSM and CUAS~~ preCICE adapters for ISSM and CUAS are described in detail.

[1] preCICE has a feature of the same name that works differently from conservative mappings in ESM couplers.

[2] Throughout the paper, we use ~~preCICE~~ preCICE terminology, where *solver* refers to a complete simulation code rather than a single numerical routine. A solver that is part of a coupled setup is referred to as *participant*. See https://precice.org/fundamentals-terminology.html.

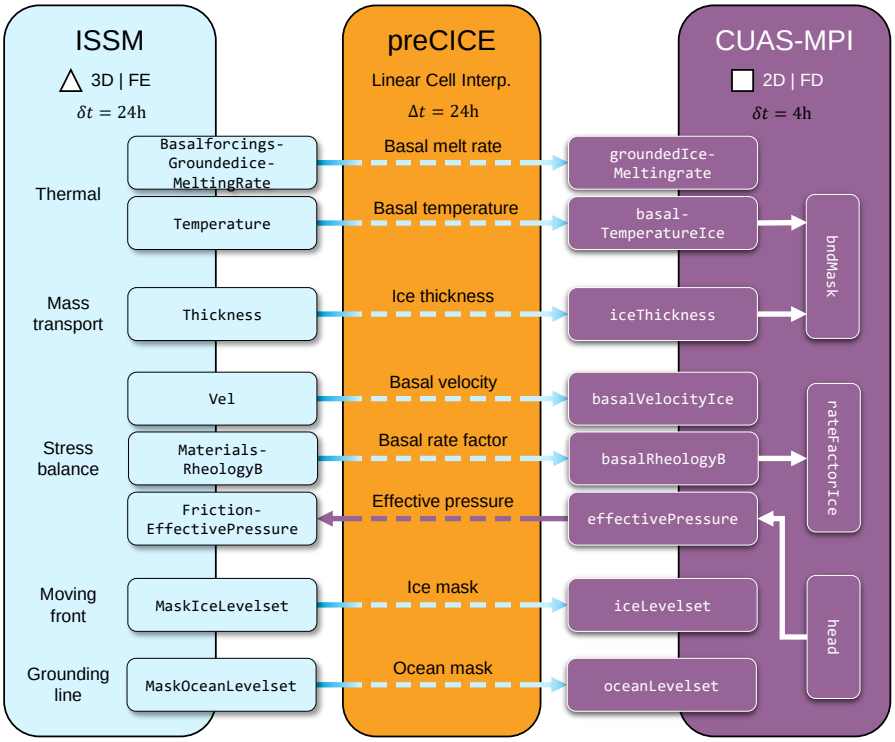

Figure 1. Overview of coupling between ~~ISSM~~ ISSM and ~~CUAS-MPI~~CUAS-MPI. The coupling library ~~preCICE~~ preCICE handles communication and data mapping between the ice sheet and hydrology models. The models are free to use their own meshes (unstructured triangular or regular rectangular) and time steps. Coupled variables are listed by the name internal to the corresponding solver/adapter. ~~ISSM~~ ISSM uses `FrictionEffectivePressure` to compute sliding. ~~CUAS~~ CUAS uses the variables received from ~~ISSM~~ ISSM as a water source and to update its active mask, see Sec. 2.4 for details. The solver and coupling configuration is described in Sec. 3

.

2.1 preCICE

~~preCICE (Precise Code Interaction Coupling Environment, Chourdakis et al., 2022)~~ The Precise Code Interaction Coupling Environment (preCICE, Chourdakis et al., 2022) is an open source coupling library for ~~multi-physics~~ multiphysics simulations. The library couples two or more independent parallel solvers (referred to as participants) and handles communication, data mapping, and coordination of the solvers, as described in the following paragraphs. Here, communication refers only to the exchange of coupling meshes and data between the solvers, not the internal parallelism of the solvers themselves. To start a coupled simulation, the user starts each solver as usual, and each solver calls the routines for initialization and data exchange of the ~~preCICE~~ preCICE library. All ~~preCICE~~ preCICE configuration options can be set ~~at runtime in a~~ in a common configuration file that is ~~shared by the participating solvers, via which the~~ read by preCICE during initialization to select the respective algorithms for communication, data mapping, and time stepping~~are selected~~. The code that connects a solver with ~~preCICE~~

preCICE (individual lines of code, a dedicated class, or a complete ~~standalone~~ stand-alone package) is called an adapter. An adapter calls the application programming interface of ~~preCICE~~preCICE, converts between the data structures of the solver and ~~preCICE~~preCICE, and steers the time evolution of the solver (i.e., adapting the time step size, or storing and reloading checkpoints, if necessary).

2.1.1 Communication

~~preCICE~~ The preCICE library communicates data between coupled solvers in a parallel, peer-to-peer, and point-to-point way. As back-ends, either TCP/IP or MPI can be used. Communication channels between the processes of both solvers are established using a highly scalable algorithm (Totounferoush et al., 2021).

2.1.2 Data mapping

To handle non-matching coupling meshes, ~~preCICE~~ preCICE offers different methods for data mapping, including projection-based methods and kernel methods (radial-basis function interpolation) (Chourdakis et al., 2022; Schneider and Uekermann, 2025). While some projection methods require mesh connectivity information, kernel methods operate solely on point clouds. Each mapping can be configured to be either *conservative* (the total values over the interface are conserved for extensive properties, e.g., mass, forces) or *consistent* (for intensive properties, e.g., temperature, pressure). ~~preCICE~~ preCICE supports 2D and 3D Cartesian meshes and surface and volume coupling. In the particular case of this paper, both codes use geographically projected coordinates and can thus apply 2D Cartesian meshes.

2.1.3 Coordination of participants

To orchestrate the simulation progress of all coupled solvers, ~~preCICE~~ preCICE offers different coupling schemes. On the one hand, ~~preCICE~~ preCICE distinguishes between serial and parallel coupling: In serial coupling, coupled solvers advance sequentially, one after the other. In parallel coupling, coupled solvers advance concurrently. In both cases, the coupled solvers synchronize and exchange data after each fixed time window. On the other hand, ~~preCICE~~ preCICE distinguishes between explicit and implicit coupling. In explicit coupling, each time window is only computed once. In implicit coupling, each time window is repeated, with modified exchanged values, until predefined convergence criteria are met. To this end, solvers need to go back in time, which is typically implemented by checkpointing in the adapter. Implicit coupling increases accuracy and numerical stability. The convergence behavior can be improved with fixed-point acceleration, for instance, with quasi-Newton methods (Mehl et al., 2016). Accuracy and numerical stability can further be improved by sampling time interpolants during each time window (Rodenberg and Uekermann, 2025). Multi-scale coupling (Desai et al., 2023) allows the coupling of macro-scale solvers with large numbers of micro-scale solvers.

2.1.4 Adapter development

Adapters for ~~some~~ several important numerical frameworks~~like OpenFOAM (Chourdakis et al., 2023)~~, such as OpenFOAM (Chourdakis et al., 2023), have been developed and are maintained by the ~~preCICE~~ preCICE team. Others are provided by the community. The ~~preCICE~~ preCICE website maintains a list of all adapters and their development status[3].

There are different ways to implement ~~preCICE adapters~~preCICE adapters[4]. Some are directly integrated or patched into the solver's code, for example~~the CalculiX-preCICE~~ , the CalculiX-preCICE adapter (Uekermann et al., 2017). Others are developed as stand-alone software packages, either as plugins like the ~~the OpenFOAM-preCICE~~ OpenFOAM-preCICE adapter (Chourdakis et al., 2023) or as orchestration codes that also call the solver like the ~~the CAMRAD II-preCICE~~ CAMRAD II-preCICE adapter (Huang et al., 2021).

2.2 ISSM

The Ice-sheet and Sea-level System Model ~~(ISSM)~~ (ISSM, Larour et al., 2012) is a well-established, feature-rich code for large-scale simulations of continental ice sheets~~(Larour et al., 2012)~~. Mathematical ice sheet models consist of balance equations for enthalpy, mass, and momentum and their respective boundary conditions and kinematic boundary conditions for geometry evolution. Ice sheet codes are typically structured in different modules, also referred to as cores, that either solve individual balance equations or deal with the processing of data into forcing fields. A highly versatile ice sheet code, such as ~~ISSM~~ISSM, offers several options for some cores. For example, the momentum balance might solve the full-Stokes equations (FS), higher-order Blatter-Pattyn approximation (HO), shallow-shelf approximation (SSA) or the shallow ice approximation (SIA), as described in the ~~ISSM~~ ISSM reference (Larour et al., 2012). Several glaciological processes can to date only be described empirically, for which a code may offer various parameterizations. Calving is such an example, for which ~~ISSM~~ ISSM offers a multitude of parameterizations. This configurability makes ~~ISSM~~ ISSM a code suitable for applications ranging from mountain glaciers ~~up~~ to continental-scale ice sheets~~but~~ , but it also leads to a large and complex code.

Most use cases of ~~ISSM~~ ISSM are large problems in the order of 0.1M - 10M degrees of freedom (DOF). For example, for simulating the Greenland Ice Sheet in moderate resolution (e.g., G4000 in (Fischler et al., 2022) with minimal element size of approximately $4\,\mathrm{km}$), the different ~~ISSM~~ ISSM cores compute 31.5k - 944k DOF, high resolution (e.g., G250 in (Fischler et al., 2022)) requires 1.1M - 32M DOF. Large problem sizes are computationally demanding, so the simulations ~~need to~~ must be efficient and scale ~~adequately~~appropriately. Fischler et al. (2022) investigated the performance of ~~ISSM~~ISSM, showing that the code scales well and is not expected to be a significant bottleneck for the scaling of the coupled simulation.

2.2.1 ~~Multi-physics~~ Multiphysics capabilities

Ice sheets are complex systems, so even a ~~standalone~~ stand-alone ice sheet simulation is already a ~~multi-physics~~ multiphysics simulation (Fig. 3). In ~~ISSM~~ISSM, the cores can be run individually, e.g., to get the stress balance solution only. However,

[3]https://precice.org/adapters-overview.html

[4]https://precice.org/couple-your-code-adapter-software-engineering.html

more often, transient runs are conducted, where most cores are solved. The system of equations of ice sheets is not solved in a numerically monolithic way, but in a sequential (segregated) fashion. In ~~ISSM~~ISSM, a typical sequence is: first, the enthalpy balance is solved, then the stress balance, and afterwards, the geometry is evolved. Each core immediately uses the results of the previous cores.

2.2.2 Mesh and solver

~~ISSM~~ISSM supports two and three-dimensional meshes. Fig. 2 shows the mesh structure. The basic horizontal two-dimensional mesh is an unstructured ~~triangle grid covering~~ triangular grid that covers the horizontal computational domain, including ice-free regions. The 2D mesh is usually static, as there is limited support for adaptive mesh refinement.

~~The horizontal 2D mesh can be used in~~ For the SSA approximation, the 2D mesh is sufficient. For HO or FS, a three-dimensional mesh is required. The 3D mesh is generated by vertically extruding the 2D mesh in multiple layers. The vertices in the top layer are ~~aligned with~~ set at the surface of the ice. The vertices in the bottom layer are set at the base of the ice. The vertices in the layer in between are ~~commonly distributed equally~~ distributed between the top and bottom vertices, ~~but may be unequally distributed as well~~often with smaller spacing at the base. Therefore, the vertical (z) coordinate of the vertices changes in every time step as the thickness of the ice changes. The vertices are connected as truncated triangular prisms or tetrahedra.

~~ISSM~~ISSM uses the finite element method (FEM) to solve the partial differential equations (~~PDE~~PDEs) for each core. The finite element type used can be configured for most cores individually. Linear P1 elements, where nodes are placed exclusively at the vertices, ~~is~~ are the default for many cores, but ~~higher order~~ higher-order elements are available.

All cores use the same mesh but generally do not have the same finite element types. The time stepping method and step size are also generally identical for every core with fixed or adaptive time steps, but a few cores, e.g., the hydrology core with the DoCo method (de Fleurian et al., 2016), subdivide the steps further. All cores use the same number of CPUs and the same domain decomposition for MPI parallelization. Fischler et al. (2022) showed that the cores that solve two-dimensional problems (e.g., mass transport, moving front) are significant bottlenecks for scaling as they compute fewer DOFs than the three-dimensional cores (e.g., thermal, stress balance). ~~This is one of the drawbacks of integrating different models into one code that coupling libraries improve upon.~~

2.2.3 Architecture

~~ISSM~~ISSM's architecture is well-suited for the development of a generic coupling adapter. Mesh and data access can be implemented based on abstract interfaces for different cores, mesh types, finite element types, etc. Variables are identified by runtime values (strings externally, mapped to enum values internally). With few exceptions~~that will be~~, noted when describing the adapter in Sect. 2.3, the adapter does not need to include code to handle specific configurations.

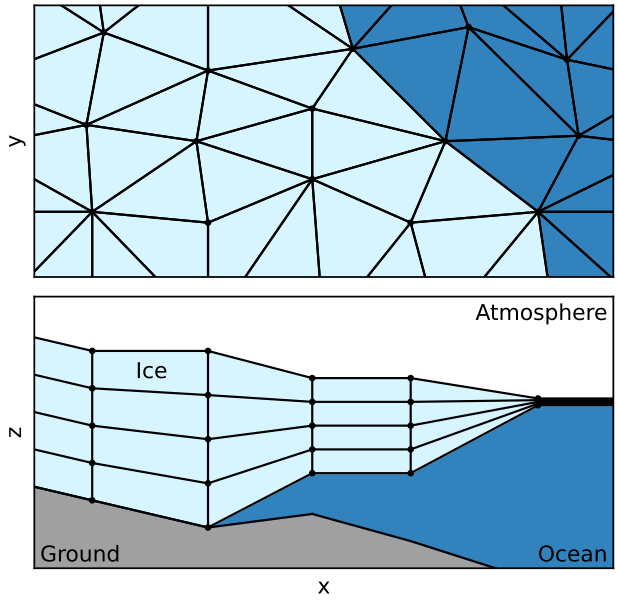

Figure 2. Schematic diagram of the ~~ISSM~~ ISSM mesh for 2D and 3D setups. The 2D mesh is an unstructured triangle grid covering the whole domain in the horizontal direction, even where there is no ice (top). Triangle elements are completely ice or completely ocean. The 3D mesh is generated by extruding the 2D mesh in multiple layers of triangle prism elements (bottom). The vertices in every layer have the same x and y coordinates. The z coordinate is set ~~so that~~ to match the ~~mesh always matches the~~ ice's vertical extent ~~of the ice,~~ and ~~it~~ is updated when the ~~thickness of the~~ ice thickness changes. In ice-free areas~~without ice~~, the mesh collapses ~~in the vertical direction~~ vertically to a ~~minimal~~ minimum thickness.

2.3 The ISSM-preCICE adapter

The ~~ISSM-preCICE~~ ISSM-preCICE adapter aims to be generic and extensible in order to support different use cases. This section explains how the features of ~~ISSM and preCICE~~ ISSM and preCICE are handled in the implementation. The adapter is an executable that runs in place of the ~~ISSM~~ ISSM executable. The adapter configuration file is specified as a command-line parameter, and the command-line parameters of the ~~ISSM~~ ISSM executable are part of the adapter configuration file. The configuration of the adapter is done by a file in YAML format. The adapter configuration file is mostly responsible for mapping names specified in the ~~preCICE~~ preCICE configuration file to names expected by ~~ISSM~~ ISSM and defining the coupling interface. Listing 1 shows an example configuration file. The format conforms to the adapter configuration schema defined by the preECO project[5]. Details of the entries in the file are explained in the following sections. Each section highlights limitations and missing features.

[5]https://precice.org/couple-your-code-adapter-software-engineering.html

```yaml
precice_config_file_name: precice-config.xml
participant_name: ISSM
issm:
  root_path: some/path/to/model
  model_name: model
interfaces:
  - mesh_name: ISSM-Mesh
    patches:
      - Base # or Surface
    read_data:
      - name: effectivePressure
        solver_name: FrictionEffectivePressure
    write_data:
      - name: iceThickness
        solver_name: Thickness
      - # ...
```

Listing 1. Example adapter configuration file in YAML format. The adapter requires information about the preCICE and ISSM configurations, the coupling mesh and the names of the variables being read or written. Variable names in the preCICE configuration file are mapped to variables known to ISSM.

2.3.1 Architecture of the adapter

Sect. 2.1.4 outlines the different ways to implement ~~preCICE~~ preCICE adapters. As shown in Fig. 3, the ~~ISSM~~ ISSM adapter is implemented as a coordinating wrapper application that calls ~~ISSM~~ ISSM (used as a library) as well as ~~preCICE~~preCICE. This approach allows for independent development and a clean architectural separation between solver and adapter, allowing, e.g., easy support for multiple ~~ISSM~~ ISSM versions. However, this relies on a relatively stable API of ~~ISSM~~ ISSM and might pose maintenance challenges in the future. Additionally, due to the architectural choice of using ~~ISSM~~ ISSM as a library (instead of via its command-line interface), some functionalities internal to ~~ISSM~~ ISSM are not available. Note that so far, no changes to ~~ISSM~~ ISSM or its build process were necessary to support the features of the adapter.

2.3.2 Coupling mesh

Since ~~ISSM~~ ISSM could potentially be coupled with many different codes, the coupling interface is configurable. The most important interfaces for coupling with the environment of the ice are the base and surface. So far, these are the only supported interfaces, see the list of limitations below for other interfaces that may be added later. In the configuration file, the user specifies which part of the mesh forms the coupling interface. The vertices of this part of the mesh are passed to ~~preCICE~~preCICE. Mesh

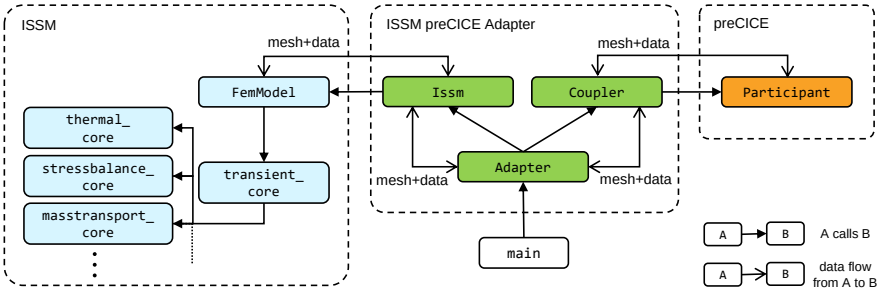

Figure 3. Structure of the ~~ISSM-preCICE~~ ISSM-preCICE adapter. The adapter has its own time loop and calls the ~~ISSM~~ ISSM solver through the ~~ISSM~~ ISSM `FemModel` class. No interaction with the internals of ~~ISSM~~ ISSM (such as the constituent cores that make up the transient core) is necessary. The `Adapter` class is the entry point of the program; it coordinates the coupling and the exchange of coupled data (read and write) between ~~ISSM~~ ISSM and ~~preCICE~~preCICE. Both ~~ISSM~~ ISSM and ~~preCICE~~ preCICE are wrapped in the adapter library to improve isolation and testability.

connectivity is added to support mapping schemes like linear cell interpolation[6] ~~(Chourdakis et al., 2022)~~(Martin, 2022). The finite element representation of ~~ISSM~~ ISSM variables is evaluated at the mesh vertices before writing data to ~~preCICE~~preCICE.

Some precision of high-order finite element types is lost when evaluating variables at the mesh vertices. Instead, the nodes of the finite elements could be used. For best results, this would require multiple coupling interfaces for different finite element types, and mesh connectivity would not be available. The adaptive mesh refinement feature of ~~ISSM~~ ISSM is not supported; the mesh must be static. Note that ~~preCICE~~ preCICE does provide facilities for mesh refinement[7], but the adapter does not yet use them.

Specialized ESM coupling support masking of irrelevant areas, e.g., masking land for ocean models. As mentioned above, ~~preCICE~~ preCICE does not provide this feature. Additionally, ~~preCICE~~ preCICE does not handle non-matching domains very well. This is not a big issue for the use case discussed here, since ~~ISSM and CUAS~~ ISSM and CUAS are interested in approximately the same domain, and both have internal mechanisms to exclude irrelevant areas and avoid wasteful computations. But it may be beneficial for, e.g., ice-ocean coupling to only couple over floating ice or coupling with a global atmosphere model.

3D (volume) coupling is a possible future extension. This would allow, e.g., to couple ~~ISSM~~ ISSM with itself to use different meshes for different cores to optimize precision or performance or to use an external thermal solver. However, as ice is transported by the solver, the z coordinate of the vertices changes in every time step. As the interface changes significantly over time, the coupling mesh could be reset to the new locations of the interface, just like for adaptive mesh refinement above. So far, we have not tested whether the computational overhead to update the coupling mesh and corresponding mapping matrices in ~~preCICE~~ preCICE is acceptable.

[6]https://precice.org/configuration-mapping.html
[7]https://precice.org/couple-your-code-moving-or-changing-meshes.html

2.3.3 Variables

In ~~ISSM~~ISSM, every state variable is identified by a unique name. These names do not follow any consistent convention, and the other coupling participant may use different names. So, it is necessary to map between names in the ~~preCICE~~ preCICE configuration file and ~~ISSM~~ ISSM names. The configuration file provides such name mappings for read and written variables.

If the ~~ISSM~~ ISSM setup uses a 3D mesh, the adapter can perform depth-averaging of a variable before writing it and extruding a variable (i.e., copying the variable values to the other layers of the mesh) after reading using the existing ~~ISSM~~ ISSM functionality.

~~ISSM~~ ISSM accepts time series as input variables. For example, the user can set specific values for these variables at the beginning, middle, and end of the simulation. ~~ISSM~~ ISSM calls these "transient variables" and temporally interpolates between these values when necessary. However, ~~ISSM~~ ISSM does not allow overwriting the user-provided values of such transient variables. Therefore, the adapter requires coupled variables to be set up as non-transient, i.e., with one fixed value that is overwritten with the value read from ~~preCICE~~ preCICE during the simulation. This is a purely technical restriction and does not reduce ~~modelling~~ modeling capabilities, since coupling also models input variables that change over time.

2.3.4 Data initialization

In ~~ISSM~~ISSM, most variables are not zero as the simulation starts at some point in time in a defined state. For some variables, e.g., ice thickness, zero is not even valid at all. For non-zero initial values, ~~preCICE~~ preCICE requires data initialization[8] by writing variables once at the beginning of the simulation. The ~~ISSM~~ ISSM adapter assumes that such initialization is necessary for every variable it writes.

For most variables, the adapter can simply write the initial value specified in the ~~ISSM~~ ISSM setup. However, users of ~~standalone ISSM~~ stand-alone ISSM are not required to specify true initial values for variables that are computed by ~~ISSM~~ ISSM before they are used. For velocity, the initial value in the setup is merely used as an initial guess for the non-linear iteration of the stress balance core. Other variables, like rheology parameter B that is computed by the thermal core, do not need to be specified in the setup at all when the corresponding core is active.

For selected variables, the adapter can be configured to compute the true initial value. For example, to initialize velocity, the adapter would run the stress balance core once. But this is not possible for every variable, at least not in a generic way, so proper initial values must be provided by the user of the adapter even when it is not required by ~~ISSM~~ ISSM itself.

2.3.5 Boundary conditions

~~ISSM~~ ISSM can set discrete Dirichlet boundary conditions (mainly called single point constraints in ~~ISSM~~ISSM) for some cores, e.g., velocity (`Vx`, `Vy`, `Vz`) in the stress balance core. The adapter has limited support to set some of these constraints by coupling. In the ~~ISSM~~ ISSM code, the constraints are stored differently from normal variables, so generic support for all constraints that ~~ISSM~~ ISSM uses is currently not possible. The association between constraints and the core that they apply to

[8] https://precice.org/couple-your-code-initializing-coupling-data.html

has to be hard-coded for each one. For example, the adapter has no way to find out automatically that constraints on velocity are used by the stress balance core. Further complicating the implementation is that manual MPI communication is required in the adapter to synchronize constraints on ghost vertices. For variables, no such extra communication was necessary.

Constraints can currently only be coupled for P1 finite elements. Internally to ~~ISSM~~ISSM, constraints are stored per finite element node, not per mesh vertex. But the coupling mesh is defined at the vertices instead of at the finite element nodes. Supporting constraints on other finite element types would require manual interpolation, whereas for normal variables, the interpolation from different finite element types is handled by ~~ISSM~~ ISSM automatically. Additionally, only velocity and pressure constraints of the stress balance core have been implemented so far.

2.3.6 Time stepping

~~ISSM~~ ISSM performs multiple time steps per coupling window, depending on the step size set in the ~~ISSM~~ ISSM setup. During a coupling window, the adapter does not perform subcycling as it is defined by ~~preCICE~~preCICE, i.e., it does not read or write intermediate values, only snapshots at the beginning or end. So, coupled variables are constant over one coupling window. The time interpolation features of ~~preCICE~~ preCICE mentioned in Sect. 2.1.3 are not currently used. This may be added in the future, but would probably require changes to the ~~ISSM~~ ISSM code. In the current version, the coupling window has to be set short enough to capture the dynamics of the system.

Implicit coupling is not supported. The adapter does not create the necessary checkpoints of ~~ISSM~~ISSM, neither in memory nor on disk. Implicit coupling is required for numerical stability in some setups (see Sect. 2.1). Our experiments show no instability with explicit coupling. This is consistent with the internal explicit coupling of ~~ISSM~~ ISSM cores explained in Sect. ~~??~~2.2.1. This is another possible future extension.

2.4 CUAS and the CUAS-preCICE adapter

~~CUAS~~ CUAS-MPI (Fischler et al., 2023) is the ~~MPI parallel~~ MPI-parallel implementation of the Confined-Unconfined Aquifer System (~~CUAS~~CUAS) model for subglacial hydrology (Beyer et al., 2018). It employs an equivalent porous medium approach (e.g., Teutsch and Sauter, 1991), in which both ~~a distributed and channelised system are represented by one~~ distributed and channelized drainage are represented within a single porous layer. The model solves a vertically integrated groundwater equation (Fischler et al., 2023, Eq. 1) using effective quantities for storativity and transmissivity, which evolve ~~over time based on parameterisations (Fischler et al., 2023, Eqns.2–4). CUAS~~ based on parameterizations (Fischler et al., 2023, Eqns.2–4). CUAS uses a finite difference spatial approximation on a regular rectangular grid and an implicit Euler time stepping scheme. ~~CUAS~~ CUAS solves for the hydraulic head that is proportional to the water pressure. The effective pressure, N (ice overburden pressure minus water pressure), is a diagnostic quantity that is computed ~~in~~ at each time step and is used in ~~ISSM~~ ISSM for sliding.

We added an experimental ~~preCICE adapter to CUAS~~preCICE adapter to CUAS. An adapter configuration file has not been specified yet, so the adapter is specific for coupling with ~~ISSM~~ISSM. The adapter currently does not support implicit coupling schemes. It is implemented within the ~~CUAS~~ CUAS code base and is not a ~~standalone~~ stand-alone application. This

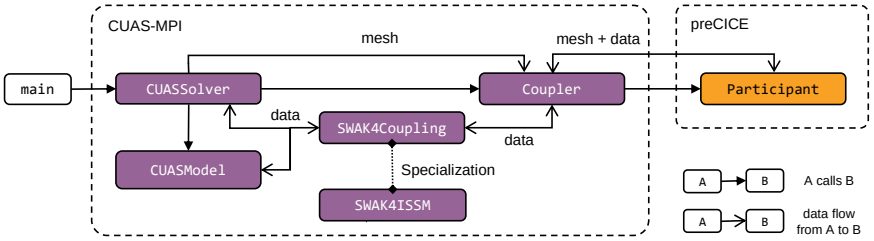

Figure 4. Structure of the ~~CUAS-preCICE~~ CUAS-preCICE adapter. The coupling is integrated into and coordinated by the existing `CUASSolver`, but most of the coupling logic is isolated in added classes. The coupling data that is read and written flows through a utility class (specialized for coupling with ~~ISSM~~ISSM) that handles transformations such as deriving ice pressure and transforming units.

implementation approach is similar to, e.g., the ~~CalculiX-preCICE~~ CalculiX-preCICE adapter (Uekermann et al., 2017) and offers a high degree of flexibility. Additionally, the code base of ~~CUAS~~ CUAS is much smaller and more modern than ~~of ISSM~~that of ISSM, so maintenance is not significantly impacted by this choice.

Fig. 4 shows an overview of the module structure and data flow. ~~preCICE~~ preCICE is integrated directly into the existing ~~CUAS~~ CUAS time step iteration, enabling subcycling and time interpolation. The ~~CUAS-preCICE~~ CUAS-preCICE adapter consists of two parts. The `Coupler` class coordinates the main coupling operations of initialization, reading and writing data, and advancing the coupling window. It exchanges data with the ~~CUAS~~ CUAS model and solver through the `SWAK4Coupling` interface, which applies necessary transformations to the data based on the model physics. While some transformations are generic, e.g., deriving ice pressure used by ~~CUAS~~ CUAS from ice thickness provided by ~~ISSM~~ISSM, others are very specific to the data that the ~~ISSM-preCICE~~ ISSM-preCICE adapter can provide, hence the `SWAK4ISSM` specialization of the interface. Some of the tasks are as simple as converting rheology parameter B from ~~ISSM~~ ISSM to `rateFactorIce` (A) in ~~CUAS~~ CUAS using $A = B^{-3}$ (assuming a Glen's flow law exponent of $n = 3$). Others are more complex. For example, we use the ice thickness to compute the ice pressure. We further compute the pressure melting point using the ice pressure and the absolute temperature from ~~ISSM~~ ISSM to decide whether the ice is frozen at the bed or not, and adjust the mask (active versus inactive) in ~~CUAS~~CUAS. Users can configure whether the mask is allowed to change based on the simulated temperature and the temperature threshold at which it becomes active. The transformations applied to the coupling data are implemented directly in the adapter, but the motivation is similar to ~~preCICE~~ preCICE Actions[9].

Each time new data is available from ~~preCICE~~ preCICE (see Fig. 1), the ~~CUAS-preCICE~~ CUAS-preCICE adapter needs to perform several tasks, which are briefly outlined below.

- `iceThickness` is translated into ice overburden pressure using ice density.

[9]https://precice.org/configuration-action.html

- `groundedIceMeltingrate` is rescaled from $\mathrm{m/s}$ ice equivalent (IE) to $\mathrm{m/s}$ water equivalent (WE) using ice and water density. This is then used as a time-independent (steady) forcing for ~~CUAS~~ CUAS during the duration of the current coupling time window.

- Use the `iceThickness` and the steady bed elevation field from ~~CUAS~~ CUAS to compute a new `bndMask` using the flotation condition. The `bndMask` contains the information where we have active hydrology (warm base, grounded ice) and where boundary conditions need to be applied (e.g. floating ice or open ocean). Here we also initialize grid points that turned from ocean into ice and thus active ~~CUAS~~ CUAS due to grounding line advance. Grounding line retreat is also handled.

- We use `iceLevelset` to disable grounded ice areas in the ~~CUAS~~ CUAS domain that are not part of the ~~ISSM~~ ISSM domain. We do not use `oceanLevelset` in the prototype implementation of the adapter.

- `basalTemperatureIce` together with `iceThickness` is used to decide if the base is at the pressure melting point to further constrain the `bndMask` in ~~CUAS~~CUAS, if needed.

- The `basalVelocityIce` is copied over without modifications.

- Finally, `rateFactorIce` (A) in ~~CUAS~~ CUAS is computed based on `basalRheologyB`.

Because the effective pressure is computed directly in ~~CUAS~~CUAS, the adapter can provide this field for coupling without further modifications. We use `iceThickness` instead of `iceLevelset` and `oceanLevelset` provided by ~~ISSM~~ ISSM to define the `bndMask` in ~~CUAS~~CUAS. This ensures that the grounding line (GL) in ~~CUAS~~ CUAS is consistent with the local bed topography. The ~~ISSM~~ ISSM mesh resolution at a given location may be substantially coarser than the ~~CUAS~~ CUAS grid resolution. Through the ~~preCICE~~ preCICE coupler, we only receive interpolated level-set fields representing the GL position on the coarser ~~ISSM~~ ISSM mesh. Consequently, the transferred GL location may not align with the grounding line implied by the higher-resolution bed topography used in ~~CUAS~~CUAS.

To enable coupled simulations, the model capabilities of ~~CUAS~~CUAS, beyond the adapter, have been further enhanced. Simulations of the Greenland Ice Sheet require water not only from the basal melt computed by ~~ISSM~~ISSM, but also from surface runoff. Until now, there has been only one input field and a corresponding internal storage field for the combined water from all sources, used as model forcing. We added the ability to store multiple water sources that can be changed independently (by a time series from input files or by coupling) and added up when required. Various parameters, such as water and ice density, that were compile-time constants are now configurable at runtime to match the parameters set in ~~ISSM~~ISSM.

3 Experiments

This section presents experimental verification of the ~~ISSM-preCICE~~ ISSM-preCICE adapter for coupling ~~ISSM to CUAS~~ISSM to CUAS. First, we demonstrate functionality using a synthetic setup, then we analyze the performance using preexisting large-scale setups of the Greenland Ice Sheet.

3.1 Functionality

We ran simulations with a synthetic setup. The simpler geometry compared to a real-life setup allows us to verify the correctness of the implementation and study the complex behavior of the coupled system in a more controlled setting.

3.1.1 Experimental setup

We use the synthetic Thule geometry developed for the CalvingMIP project (Jordan, 2024). This setup is based on analytical functions for the bed elevation and yields an ice-sheet geometry that encompasses all major components of an ice-sheet model domain (grounded ice, floating ice, and open ocean). In CalvingMIP it is used to study how different ice sheet models handle calving in a very controlled setup. Instead of fixed thermal and friction conditions as in the original definition, we enable the thermal core of ~~ISSM~~ ISSM with surface temperature $250\,\mathrm{K}$ and geothermal flux $0.05\,\mathrm{W\,m^{-2}}$ to compute basal melt rates to be used by ~~CUAS~~ CUAS and we use the default Budd friction law ($\boldsymbol{\sigma}_b = -C^2 N^{\frac{q}{p}} |\boldsymbol{v}_\mathrm{b}|^{\frac{1}{p}-1} \boldsymbol{v}_\mathrm{b}$) with coefficient $C = 100$, exponents $p = 3$ and $q = 2$, and effective pressure N supplied by ~~CUAS~~CUAS. Surface mass balance was increased to $8\,\mathrm{m/a\,IE}$. The goal is to have a balanced geometry with grounded and floating, fast- and slow-flowing regions to assess the effects of coupling.

The combined model (~~ISSM~~ ISSM + ~~CUAS) initialization~~ CUAS) spin-up consists of two phases. First, we run the ~~ISSM~~ ISSM model for 12,000 years with a time step of $0.1\,\mathrm{a}$ to reach a steady state, using an effective pressure equal to the ice overburden pressure. In the second phase, ~~CUAS and ISSM~~ CUAS and ISSM run coupled without melt runoff forcing, exchanging data every $0.1\,\mathrm{a}$ (equal to the ~~ISSM~~ ISSM time step) for $200\,\mathrm{a}$. This allows ~~CUAS~~ CUAS to find its own steady state while keeping ~~ISSM~~ ISSM state consistent with the effective pressure computed by ~~CUAS~~CUAS.

For the actual experiment, we add forcing in the form of seasonal and spatially varying meltwater runoff (in addition to the basal meltwater received from ~~ISSM) to CUAS~~ ISSM) to CUAS to induce a dynamic system. We ran simulations with low and high runoff. The peak forcing in summer (day 210 of the year) in areas with ice surface below $500\,\mathrm{m}$ is $0.2\,\mathrm{m/a\,WE}$ for low runoff and $2.0\,\mathrm{m/a\,WE}$ for high runoff. Over the year, the forcing follows the shape of a Gaussian distribution with parameters $\mu = 210\,\mathrm{d}$ and $\sigma = 20\,\mathrm{d}$. Spatially, forcing is maximal ~~for ice surface~~ in areas of low ice surface elevation ($h_\mathrm{s} < 500\,\mathrm{m}$~~, zero~~) and zero in areas of high ice surface elevation ($h_\mathrm{s} > 1500\,\mathrm{m}$~~, and in between~~). For medium ice surface elevation, forcing follows a monotone cosine curve, i.e., ~~forcing increases~~ it increases continuously as the surface elevation decreases. The surface elevation h_s is taken at the end of the spin-up, the forcing is not dynamically updated.

The basic coupling configuration, both for spin-up and the following experiment, is shown in Fig. 1. As described above, ~~CUAS~~ CUAS writes the effective pressure that is used by ~~ISSM~~ ISSM to determine basal friction. The basal melting rate from ~~ISSM~~ ISSM provides a water source for ~~CUAS~~CUAS. Basal temperature, ice thickness, and ice and ocean masks are used to update the active ~~CUAS~~ CUAS mask. The temperature threshold for activating the mask is set to $269.15\,\mathrm{K}$. Ice velocity and rheology govern channel opening and closure, represented in CUAS by increasing and decreasing transmissivity, respectively. We use linear cell interpolation to map data between the two meshes. Details on how the coupled variables are used in ~~CUAS~~ CUAS are described in Sect. 2.4. Simulations are run over two years to assess changes from one year to the next. Data is

exchanged daily to accurately capture rapid changes during summer. ~~ISSM~~ ISSM uses time steps of 1 d same as the coupling window, ~~CUAS~~ CUAS 4 h.

We compare a fully coupled (2-way) run with one in which coupling is performed only in one direction (1-way). In 2-way, ~~ISSM and CUAS~~ ISSM and CUAS exchange all variables as per the coupling configuration described above. In 1-way, ~~ISSM~~ ISSM receives the updated effective pressure from ~~CUAS, but CUAS~~ CUAS, but CUAS does not receive updated ice geometry from ~~ISSM~~ISSM. This is equivalent to offline coupling: first run ~~CUAS standalone~~CUAS stand-alone, then use the resulting time series as input for a ~~standalone ISSM~~ stand-alone ISSM simulation. To ensure comparable aggregate forcing, ~~CUAS~~ CUAS receives the steady basal melt field from the end of the spin-up from an input file.

3.1.2 Results

The state at the end of the combined model initialization (spin-up) is presented in Fig. 5. The ice thickness and basal velocity are selected as the key quantities describing the ice sheet state, while effective pressure and subglacial discharge are selected to describe the state of the subglacial hydrology. The dark gray areas in Fig. 5a–d (and subsequent maps) indicate the grounded parts of the domain where basal temperatures from ~~ISSM~~ ISSM are below the pressure melting point, and ice sheet basal melt is zero (cold base) and hence no active hydrology exists. The ice thickness (Fig. 5a) in the ~~warm based~~ warm-based area varies over several thousand meters, with low thickness in region A and along the northern and southern grounding lines, as well as the upstream end in region B. The effective pressure (Fig. 5b) is lowest at the grounding line and reaches magnitudes above 6 MPa. Basal velocities (Fig. 5c) range from 10 to about 400 m/a with the largest values along the long grounding lines in the north and south. Along those grounding lines, the subglacial discharge (Fig. 5d) is highest, with a similar pattern of N, v_b and D.

For a further investigation of the differences in 1- and 2-way coupling, we present simulations with different magnitude in seasonal forcing. Figure 6 displays the time series of total water source, Q_tot, mean effective pressure, $\bar{N}$, mean effective transmissivity magnitude, $\overline{\log(T_\mathrm{e})}$, and ~~masal~~ basal velocity magnitude, $\overline{\log(v_\mathrm{b})}$ showing 1-way and 2-way coupling and for each full forcing (high) and only 10% amplitude forcing (low). The imposed runoff forcing is periodic with a one-year period and attains its maximum at day 210, end of July. As model output is written every 10 days, this maximum is not sampled exactly in the second simulation year. The nearest stored time step (day 215)~~therefore~~ , therefore, exhibits a slightly reduced signal amplitude. The effective pressure (Fig. 6b) has a lower difference between 1- and 2-way coupling for low runoff forcing. In both runoff cases, the 2-way coupling has higher $\bar{N}$. The timing in $\bar{N}$ is ~~in the low runoff forcing is~~ slightly delayed to Q_tot due to the low runoff forcing. The timing of $\overline{\log(T_\mathrm{e})}$ (Fig. 6c) in the low runoff forcing is similar to $\bar{N}$ and $\overline{\log(v_\mathrm{b})}$ (Fig. 6d). The effect of the coupling is small for low runoff forcing in $\overline{\log(T_\mathrm{e})}$, with larger differences outside the peak runoff and higher $\overline{\log(T_\mathrm{e})}$ in 1-way. The basal velocity resembles the inverse shape of $\bar{N}$.

Comparing the results for 1-way and 2-way coupling in ice thickness difference (Fig. 7a, 8a), we find distinct differences in the regions A and B: in A the 1-way case exceeds ±50 m, while the 2-way case has small differences. The pattern of ice thickness difference is similar for the ~~1-~~1-way and 2-way coupling, but the magnitude is significantly larger in the 1-way case~~by far larger~~. For both ~~,~~1-way coupling and 2-way coupling, we find a reduction in effective pressure compared to the

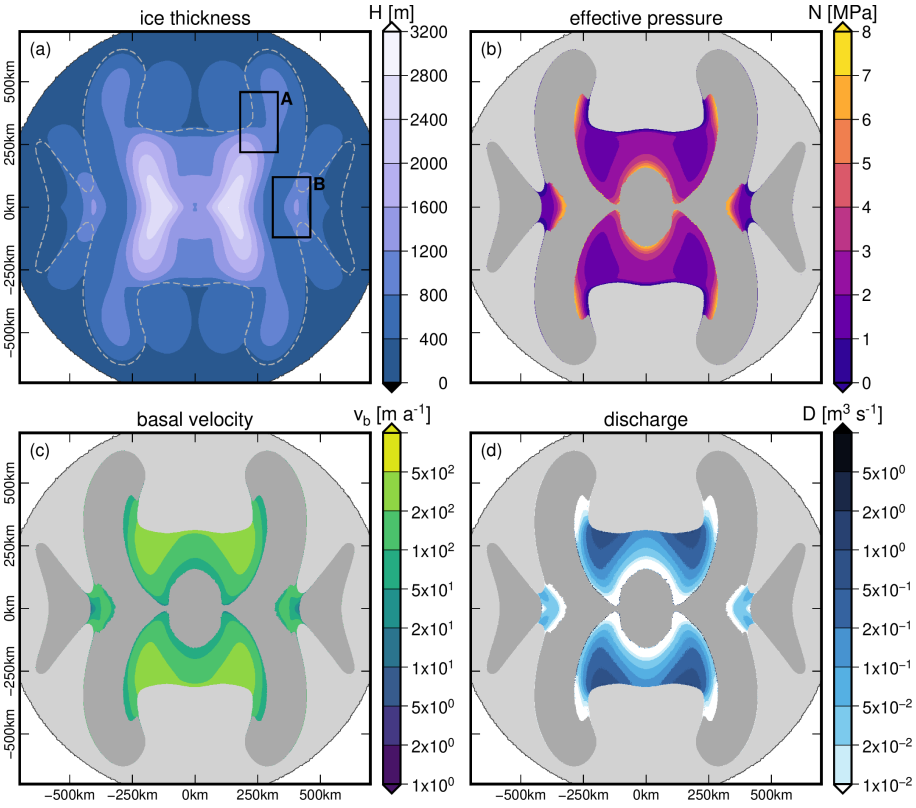

Figure 5. Model state at the end of the spin-up for the Thule domain setup. Ice-dynamical fields are shown in the left column: (a) ice thickness and (c) basal velocity. Subglacial hydrological fields are shown in the right column: (b) effective pressure and (d) subglacial discharge. ~~Colored shading~~ Ice thickness in (a) is shown over the full plotted extent, while all other fields are shown only for the grounded ~~portion of the~~ ice ~~sheet;~~ area. The grounding line is indicated in (a) by a dashed line. In panels (b–d), floating ice shelves are ~~indicated~~ shown in light gray~~. Dark~~ , and dark gray areas indicate grounded regions that are inactive in ~~CUAS~~CUAS. The maps are cropped relative to the full computational domain to focus on the grounded ice region~~and therefore do not display the full computational domain~~. Rectangles (A, B) indicate regions of high activity referenced in the text.

spin-up that does not contain seasonal runoff (Fig. 7b, 8b). ~~The basal velocity is in both cases,~~ In both 1-way ~~coupling~~ and 2-way coupling, we have an increase in basal velocity compared to the spin-up (Fig. 7c, 8c), with an extreme increase in region A for the 1-way coupling. The discharge (Fig. 7d, 8d) is in both cases larger than in the spin-up, but the difference to the spin-up is only moderate in magnitude, except for region B in the 1-way case.

3.2 Performance

The coupled simulation should run with minimal computational overhead and use computing resources efficiently. To demonstrate this, we use a large-scale setup of the Greenland Ice Sheet as the simple setup used in Sect. 3.1 is not complex enough

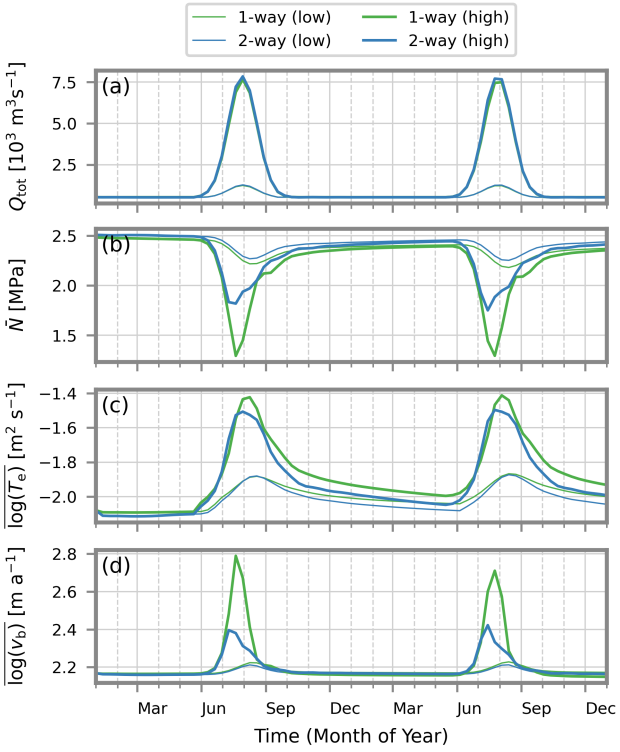

Figure 6. Time series of total water source Q_{tot}, mean effective pressure $\bar{N}$, mean effective transmissivity magnitude $\overline{\log(T_e)}$, and mean basal velocity magnitude $\overline{\log(v_b)}$ for the four simulations: one-way coupling in green, two-way coupling in blue; high-amplitude forcing shown with thick lines, low-amplitude forcing with thin lines. The means are evaluated as spatial means on the time-dependent active ~~CUAS~~ CUAS mask.

to have performance characteristics that are representative of real uses cases, which usually have much more complexity. We have analyzed the performance of initialization and data mapping, as well as scaling with the number of processes.

3.2.1 Experimental setup

The setup for ~~ISSM~~ ISSM is mostly the same as G1000 in Fischler et al. (2022). The only modification we made for this paper is to use the default ~~ISSM~~ ISSM Budd friction law $\boldsymbol{\sigma}_b = -C^2 N^{\frac{q}{p}} |\boldsymbol{v}_b|^{\frac{1}{p}-1} \boldsymbol{v}_b$ with coefficient $C = 12.94$, exponents $p = 3$ and $q = 2$, and effective pressure N provided by ~~CUAS~~CUAS. The spin-up process is the same as in Fischler et al. (2022). During the spin-up, the effective pressure is $N = N_{\mathrm{opc}} = \rho_{\mathrm{ice}} g H - \max(0, \rho_{\mathrm{water}} g(-z_b))$ with z_b the height of the base above sea level as in Wolovick et al. (2023). The setup set the lower bound for effective pressure 35 % of ice overburden pressure. This parameter is likely to affect the stability of the coupled system, but investigating its effect in detail is beyond the scope of this work. The resolution of the mesh is around $0.7\,\mathrm{km}$ at the shear margins, $10\,\mathrm{km}$ at slow-moving ice in the interior, and up to $100\,\mathrm{km}$ at open ocean.

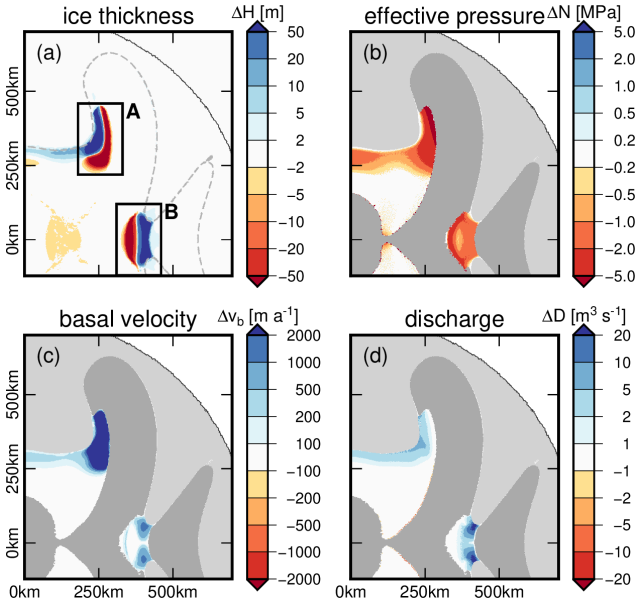

Figure 7. ~~Result~~ Results of the one-way coupled simulations using the Thule setup. ~~The panels a–d~~ Panels (a–d) show ~~the~~ differences ~~of~~ in the summer state (day 215 ~~in the second~~ of year two) ~~with respect~~ relative to the end of the spin-up. The panel layout is identical to Fig. 5, with ice-dynamical fields in the left column (a,c) and subglacial hydrological fields in the right column (b,d). Differences are evaluated on the common grounded domain, except for panel (a), where ice thickness differences are shown wherever ice thickness is defined. The maps ~~are cropped to~~ show approximately one quarter of the ~~northern part~~model domain, ~~the missing southern part is symmetrical~~exploiting symmetry along both horizontal axes. Rectangles (A, B) indicate regions of high activity referenced in the text.

The ~~CUAS~~ CUAS setup is taken from Fischler et al. (2023). We use G600, which has a uniform grid with $600\,\mathrm{m}$ resolution, similar to the minimum element size of the ~~ISSM~~ ISSM mesh. We use daily surface runoff data (R) from the regional climate model RACMO (Noël et al., 2019) for the year 2019 in addition to the ice sheet basal melt (M) from ~~ISSM~~ ISSM to impose seasonality to the ~~CUAS~~ CUAS water source as:

$$Q(x,y,t) = M(x,y,t) + 0.9R(x,y,t), \tag{1}$$

where we only consider 90% of the surface runoff to enter the subglacial system. The percentage is arbitrary, but ensures strong seasonality for the coupled simulations. In the year 2019, particularly high melt was measured for the Greenland Ice Sheet (Tedesco and Fettweis, 2020; Sasgen et al., 2020). The aquifer layer thickness in ~~CUAS~~ CUAS was chosen equal to 1 m, with yield storativity $S_y = 10^{-2}$ and minimal transmissivity $T_{\min} = 10^{-14}\,\mathrm{m}^2/\mathrm{s}$. Subglacial channel creep opening/closure is parameterized using an ice flow rate factor of $A = 6.8 \times 10^{-24}\,\mathrm{Pa}^{-3}\,\mathrm{s}^{-1}$ (Werder et al., 2013). All remaining parameters are unchanged from those reported in Fischler et al. (2023). For defining the initial active mask in ~~CUAS~~CUAS, a threshold of minimum 10 m of ice thickness was chosen. The temperature threshold for activating the mask during simulation is set to $269.15\,\mathrm{K}$. Similar to ~~ISSM~~ISSM, the initial hydraulic head of ~~CUAS~~ CUAS is derived from N_{opc}.

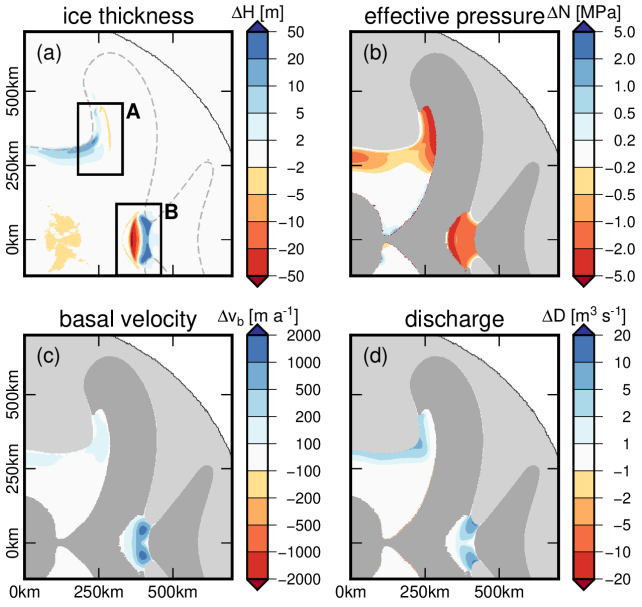

Figure 8. Result of the fully coupled (two-way) simulations using the Thule setup. ~~The panels a–d~~ Panels (a–d) show ~~the~~ differences ~~of~~ in the summer state (day 215 ~~in the second~~ of year two) ~~with respect~~ relative to the end of the spin-up. The panel layout is identical to Fig. 5, with ice-dynamical fields in the left column (a,c) and subglacial hydrological fields in the right column (b,d). Differences are evaluated on the common grounded domain, except for panel (a), where ice thickness differences are shown wherever ice thickness is defined. The maps ~~are cropped to~~ show approximately one quarter of the ~~northern part~~model domain, ~~the missing southern part is symmetrical~~exploiting symmetry along both horizontal axes. Rectangles (A, B) indicate regions of high activity referenced in the text.

The ~~preCICE~~ preCICE coupling configuration is the same as in Sect. 3.1 with the exception of using different mapping methods for Sect. 3.2.4 and different coupling schemes for Sect. 3.2.3. Simulations run for 730 days.

For the measurements, we are using the profiling utility integrated into ~~preCICE~~preCICE[10]. ~~Runtime~~ The runtime of initialization is measured at the beginning. Where we report aggregate runtime of solvers or data mapping in the following sections, only the final 365 days are included. This ensures that the analysis includes a full year of seasonal changes but excludes the noisy early-coupling windows in which the states of ~~ISSM and CUAS~~ ISSM and CUAS are not yet aligned. In real use, depending on which parameters are changed between runs, this relaxation phase could be skipped entirely by using restart files. Runtime measurements do not include writing output, as I/O execution times can swing wildly and unpredictably. Adding moderate amounts of data output to both participants should not, on average, significantly impact the analysis. Every experiment is repeated three times, and the results are averaged to reduce variance.

In parallel coupling schemes, every participant has its own exclusive resources. CPUs are assigned according to a ratio $\alpha = n_{\mathrm{ISSM}}/n_{\mathrm{CUAS}}$ where n_{S} is the number of CPUs assigned to solver S. Care is taken to assign packed CPU blocks to

[10]https://precice.org/tooling-performance-analysis.html

participants, i.e., processes used by one participant are as local to the nodes as possible, since each participant communicates more internally than with other participants.

In serial coupling schemes, we conducted experiments with both shared and exclusive resources. Shared resources are used by both solvers in turn. Exclusive resources are used by only one solver and are idle while the other solver computes. That means, except during initialization, half of the CPUs will be almost completely idle. ~~No~~ Little energy is wasted, but the cluster resources are nonetheless reserved for the entire run. With shared resources, both solvers always use all allocated CPUs, as it is generally recommended to use all allocated cluster resources unless the region of flat or negative scaling is reached. For better comparisons, we also allocate the same number of CPUs to both solvers when using exclusive resources.

Where we give CPU or process counts below, they have the following meanings for the coupling and resource allocation schemes:

- Parallel: total number of processes allocated to both solvers, each solver using a fixed subset.
- Serial (shared): total number of processes allocated, used by both solvers in turn.
- Serial (exclusive): maximum number of processes allocated to either solver. Since the processes of the other participant are mostly idle, this results in the most relevant comparison regarding the required resources and it allows us to measure the effect of resource contention. As both solvers use the same number of processes, the number of processes given in plots is half the number of processes allocated.

All experiments are performed on the Albedo cluster of the Alfred Wegener Institute. The compute nodes of the cluster are equipped with 256 GB of RAM and two AMD Rome Epyc 7702 CPUs for a total of 128 CPU cores per node and are connected by 100 Gb InfiniBand network. The solvers and dependencies are built with GCC version 12.1.0 and OpenMPI version 4.1.3.

3.2.2 Initialization

In ~~earth system models, initialization of the coupled setup is often a significant part of the runtime, see for example the runtime analysis of the OASIS3-MCT coupling library in Craig et al. (2017)~~Earth System Models, initialization time of the solvers and the coupling library is of significant concern. For this scaling analysis, we use nearest neighbor mapping exclusively. Comparison of mapping methods follows in Sect. 3.2.4.

Fig. 9 shows the time required to initialize ~~preCICE~~preCICE. This includes ~~both partition~~ establishing connections between participants and processes, partitioning of the domain, and computation of mapping weights. We do not analyze these parts separately, as it would require too much explanation of preCICE internals, and we are primarily working from the point of view of a preCICE user. For comparison, Fig. 10 and ~~9~~ 11 show the time required to initialize the solvers. Note that ~~ISSM and CUAS~~ ISSM and CUAS initialize at the same time, so the actual time required is the maximum of both. While the data is quite noisy due to a low number of repetitions and high variance of I/O, general trends can be identified.

~~ISSM~~ ISSM initialization time grows linearly with the number of processes. ~~CUAS~~ CUAS is basically constant, trending slightly downward. Solver initialization is dominated by ~~CUAS~~ CUAS at low CPU counts. The larger mesh means higher data input requirements. ~~ISSM~~ ISSM catches up between 1024 and 2048 processes due to less optimal parallel I/O accesses.

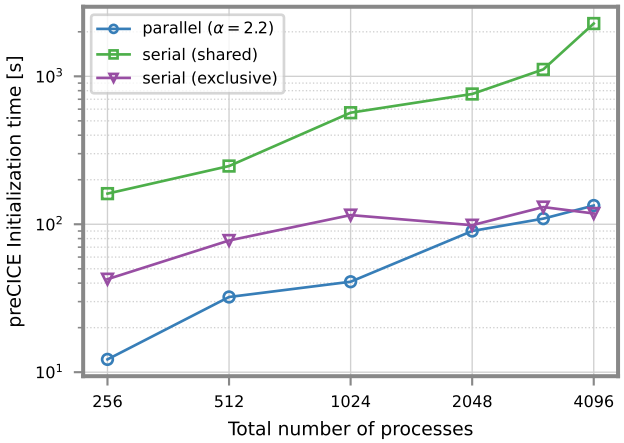

Figure 9. Time to initialize ~~preCICE~~ preCICE in the Greenland setup for different coupling and/or resource allocation schemes and increasing numbers of processes. For the parallel coupling scheme, CPUs are allocated to ISSM and CUAS at a ratio of $\alpha = n_{\text{ISSM}}/n_{\text{CUAS}} = 2.2$. The serial coupling scheme can be run with exclusive CPUs for each participant or with shared resources that are used in turn. Initialization includes partitioning of the coupling mesh and computation of nearest neighbor mapping weights for both solvers.

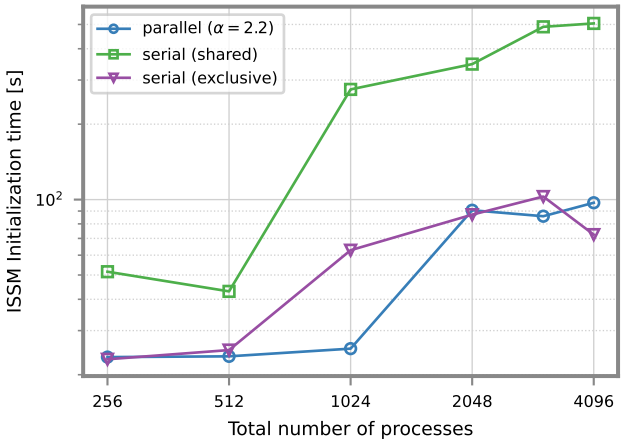

Figure 10. Time to initialize the ~~ISSM~~ ISSM Greenland setup for different coupling and/or resource allocation schemes and increasing numbers of processes. Initialization consists mostly of loading of input data from files.

In the range of CPU counts tested, ~~preCICE~~ preCICE initialization times also grow linearly with the number of processes, as more communication is necessary to partition the meshes and compute weights. Initializing the coupler and initializing the solvers ~~take similar timeexcept when sharing~~ requires similar time, except in the case of serial coupling with shared resources.

Sharing resources during initialization in serial coupling has a strong negative effect. Naive estimation would suggest the required time doubles for shared resources, since the same amount of work is being done by half the CPUs. However, scheduling conflicts can increase times by an order of magnitude or more. ~~CUAS~~ CUAS is especially badly affected, probably due to

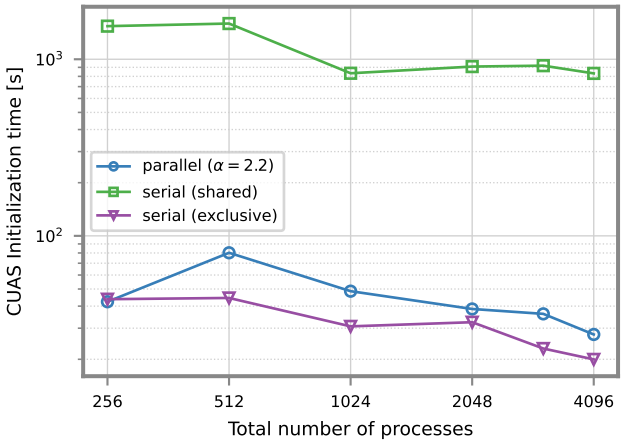

Figure 11. Time to initialize the ~~CUAS~~ CUAS Greenland setup for different coupling and/or resource allocation schemes and increasing numbers of processes. Initialization consists mostly of loading of input data from files.

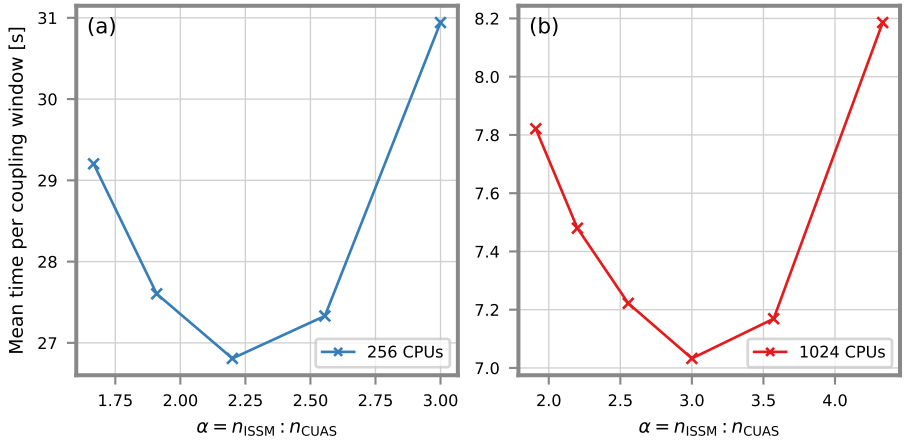

Figure 12. Average time to compute one coupling window with parallel coupling scheme in the Greenland setup for different distributions of 256 (a) and 1024 (b) total CPUs.

contention of I/O resources. Parallel and serial exclusive require approximately the same amount of time. The increased effort required to compute and communicate the weights of a more partitioned mesh is counterbalanced by the increased resources.

3.2.3 Simulation

For parallel coupling, we first needed to determine the optimal distribution of available CPUs among the solvers. This is the ratio of CPUs used by ~~ISSM and CUAS~~ ISSM and CUAS where both solvers take approximately the same time for one coupling window. Fig. ~~??~~ 12 a shows the times required to compute a single coupling window with different distributions of

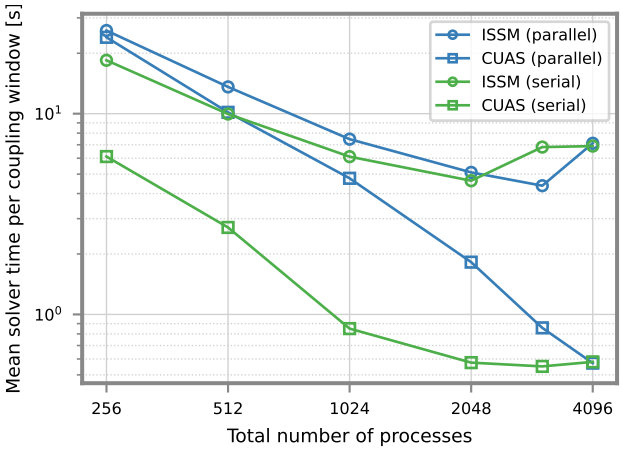

Figure 13. Average execution time required by the ~~CUAS~~ CUAS and ~~ISSM~~ ISSM solver during one coupling window for ~~CUAS~~ CUAS and ~~ISSM~~ ISSM in the Greenland setup for increasing numbers of MPI processes.

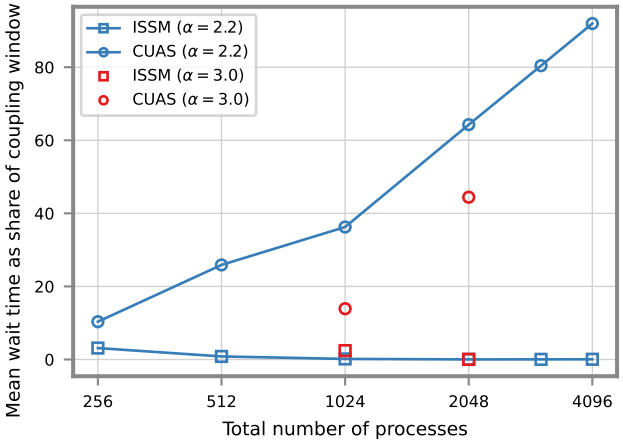

Figure 14. Average wait time relative to execution time of one coupling window for ~~CUAS~~ CUAS and ~~ISSM~~ ISSM in the Greenland setup in a parallel coupling scheme for increasing numbers of MPI processes and two different distributions of processes to participants.

256 total CPUs. The best result is at $\alpha = 2.2$. If both participants scale equally, this would be the ideal distribution for larger numbers of CPUs as well.

However, as Fig. 13 displays, ~~ISSM~~ ISSM does not scale as well as ~~CUAS~~CUAS. This is consistent with the scaling analyses of ~~standalone ISSM (Fischler et al., 2022) and CUAS~~ stand-alone ISSM (Fischler et al., 2022) and CUAS (Fischler et al., 2023) as well, even though the uncoupled and coupled solvers are not directly comparable. Accordingly, with increasing numbers of processes, the duration that ~~CUAS waits for ISSM~~ CUAS waits for ISSM increases as shown in Fig. 14. At 256 processes,

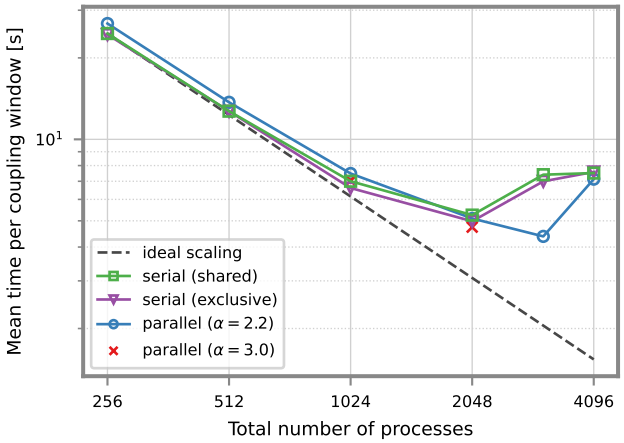

Figure 15. Average execution time for one coupling window (includes solver, communication, and data mapping) using a parallel or serial coupling scheme in the Greenland setup for increasing numbers of MPI processes. Parallel coupling is tested with different distributions of processes to participants, serial coupling with exclusive or shared resources.

where the distribution of $\alpha = 2.2$ had the best result, the wait times are close. Note that even here, the wait time is not zero, as the computational effort of each solver varies with the seasons, and both solvers wait in some coupling windows.

~~Average time to compute one coupling window with parallel coupling scheme in the Greenland setup for different distributions of 1024 total CPUs.~~

These results suggest that more than 256 CPUs should be distributed differently. Fig. ~~??~~ 12 b shows that for 1024 processes, the ideal distribution would be $\alpha = 3.0$. Fig. 14 shows reduced wait times for this distribution over $\alpha = 2.2$. Note that when running the simulation once at any moderate distribution α and measuring the average solver runtime t_{X}, the equation $\alpha_{\mathrm{opt}} = t_{\mathrm{ISSM}}/t_{\mathrm{CUAS}} * \alpha$ gives a decent approximation of the optimal distribution. For example, with $\alpha = 2.2$ and the measured solver times $t_{\mathrm{ISSM}} = 7.5\,\mathrm{s}$ and $t_{\mathrm{CUAS}} = 4.8\,\mathrm{s}$, the estimated optimal distribution is $\alpha_{\mathrm{opt}} = 3.4$, which is close to the minimum in Fig. ~~??~~12 b.

With these preparations, we ran scaling experiments of the coupled system. Fig. 15 shows a comparison of average run times for a coupling window for parallel and serial coupling schemes with different resource allocations.

In the lower range of processes, where both serial and parallel show almost ideal scaling, serial coupling is slightly faster. There is an unexpected bend in the measured times for serial coupling. The same bend is observed in the ~~ISSM~~ ISSM solver execution times, but not in ~~CUAS~~CUAS. We were unable to identify the root cause or any difference in the simulation that could explain it, the ~~numbers~~ number of solver iterations ~~are~~ is similar between all experiments. A deeper analysis of the ~~ISSM~~ ISSM solver is beyond the scope of this work. ~~It is possible that a technical aspect of the cluster interferes in the simulation with the most processes.~~

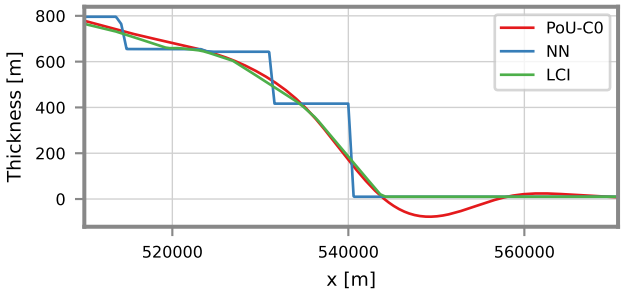

Figure 16. Results of mapping ice thickness from ~~ISSM~~ ISSM to ~~CUAS~~ CUAS mesh in the Greenland setup using different mapping methods along a horizontal section that crosses the ice boundary at $y = -1277863.4\,\mathrm{m}$. Partition-of-unity radial basis functions (PoU-C0) overshoots and produces unphysical values at the ice boundary. Linear cell interpolation (LCI) is equivalent to the P1 finite elements used by ~~ISSM~~ISSM. Nearest neighbor (NN) is constant in regions around ~~ISSM~~ ISSM vertices.

Exclusive resources for serial coupling give a small advantage over shared resources, but probably insignificant compared to the difference in initialization times discussed in Sect. 3.2.2. Scaling is basically identical. The changed distribution of CPUs in parallel coupling also gives a small advantage over the original distribution.

3.2.4 Mapping

~~preCICE~~ preCICE offers a choice of different methods for mapping data between meshes. The methods differ in the order of approximation and computational cost. We ran experiments with a selection of three methods of different order:

- nearest neighbor (NN), a first order projection method
- linear cell interpolation (LCI), a second order projection method using barycentric coordinates
- partition-of-unity radial basis functions (PoU), a kernel based method designed for large scale mappings

We tested all mapping methods with a parallel coupling scheme on 1024 total CPUs, distributed $2.2:1$ to ~~ISSM and CUAS~~ ISSM and CUAS and measured the initialization time and mapping time per coupling window.

The PoU method and basis functions must be parameterized[11]. Our setup is particularly challenging for the current, relatively recent implementation of PoU in ~~preCICE~~preCICE. As described in Sect. 3.2.1, the ~~ISSM~~ ISSM mesh has a wide range of element sizes. However, ~~preCICE~~ preCICE currently permits only a single global parameter each for the basis function radius and PoU cluster size. In addition, the fields of an ice sheet model include discontinuities at the calving front and grounding line. Even with the best parameterization we found (C0 compact polynomial basis functions, radius $200\,\mathrm{km}$ for mapping from ~~ISSM to CUAS~~ISSM to CUAS, $10\,\mathrm{km}$ from ~~CUAS to ISSM~~CUAS to ISSM, default values for the other parameters), there is overshooting, e.g., negative ice thickness values all around the ice boundary as in Fig. 16. Performance measurements are included here with the hope that improvements in ~~preCICE~~ preCICE and/or the setup will be implemented. The other methods

[11] https://precice.org/configuration-mapping.html

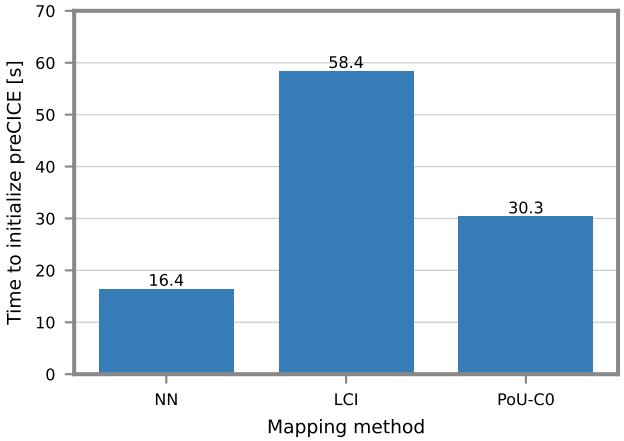

Figure 17. Time required to initialize ~~preCICE~~ preCICE for both coupling participants in the Greenland setup for different mapping methods: nearest neighbor (NN), linear cell interpolation (LCI) and partition-of-unity radial basis functions with C0 compact polynomial basis (PoU-C0). Both participants use the same mapping method, mapping is computed by the reading participant.

did not show such problems, detailed analysis of numerical errors is beyond the scope of this work but is covered in Chourdakis et al. (2022), Schneider and Uekermann (2025), and Hocks and Uekermann (2026).

Fig. 17 shows the total runtime required to initialize ~~preCICE~~ preCICE for both participants. This time includes both communication, mesh partitioning, and initializing data mappings. For all methods, initialization of ~~preCICE~~ preCICE is around the same order as initialization of the solvers (see Fig. 10 and 11). LCI is about twice as expensive as PoU and almost four times as expensive as NN.

Fig. 18 shows the runtime required to map the data in each coupling window. The cost difference between the mapping directions (~~ISSM to CUAS or CUAS to ISSM~~ISSM to CUAS or CUAS to ISSM) can be attributed to the number of fields that must be mapped. NN and LCI are very close in cost, whereas PoU is significantly more expensive. However, for all mapping methods, the runtime of a coupling window (see Fig. 15) is dominated by the solvers themselves. NN was measured at approximately $9\,\mathrm{ms}$ from ~~CUAS to ISSM~~CUAS to ISSM, $25\,\mathrm{ms}$ from ~~ISSM to CUAS~~ISSM to CUAS, or ~ 0.1 % and ~ 0.3 % of the total time of a coupling window. LCI was measured only slightly slower, at $10\,\mathrm{ms}$ (~ 0.1 %) and $29\,\mathrm{ms}$ (~ 0.4 %). Note that the difference is too small to be reliably measured with this setup. The cost of PoU, on the other hand, is not as negligible, with $58\,\mathrm{ms}$ (~ 0.7 %) and $380\,\mathrm{ms}$ (~ 6 %). The detailed profile shows a significant imbalance in the distribution of work, probably due to the uneven mesh resolution. The slowest processes work up to four times longer than the fastest.

4 Discussion

The new coupling framework presented in this paper is a promising approach for the development of coupled ice sheet and ~~earth system models~~Earth System Models. Compared to SHAKTI (Sommers et al., 2018), DoCo (de Fleurian et al., 2016), and

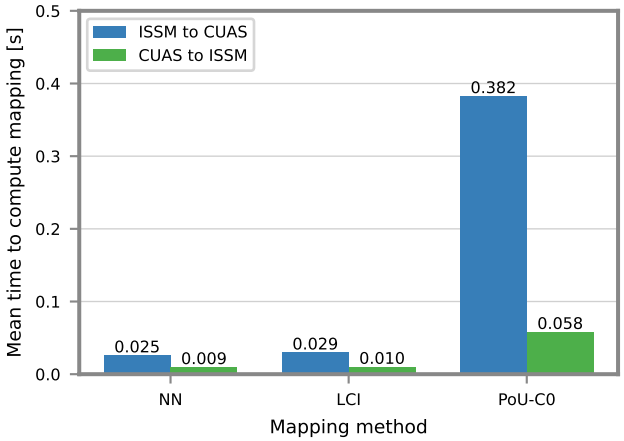

Figure 18. Time required to compute data mapping per coupling window in the Greenland setup for different mapping methods: nearest neighbor (NN), linear cell interpolation (LCI) and partition-of-unity radial basis functions with C0 compact polynomial basis (PoU-C0). Mapping is computed by the reading participant.

other hydrology models directly integrated into ~~ISSM~~ISSM, external coupling (with ~~preCICE~~ preCICE or another library, see discussion below) allows more choice of implementation and numerical treatment. Development of the models can progress independently, and neither model is restricted by the choices of the other. The effort to set up the coupling is minimal. Coupling scheme, data mapping, and coupling time window are easy to adapt and extend to additional participants.

The ~~ISSM-preCICE~~ ISSM-preCICE adapter provides the basic features necessary for most use cases. It significantly reduces the effort required to couple other codes to ~~ISSM~~ISSM, but it will almost certainly become necessary to allow the adapter to be customized more, e.g., to add logic specific to each coupling setup, such as deriving model variables as we already had to do in the ~~CUAS~~ CUAS adapter. Additionally, we listed some general limitations to be resolved in Sect. 2.3. For example, accuracy is lost because the coupling interface is based on the mesh vertices instead of finite element nodes, and it is not yet possible to couple the full three-dimensional volume of the ice sheet. Some features of ~~ISSM and preCICE~~ ISSM and preCICE are not supported at this stage, among them dynamic adaptive meshes and time interpolation. It was not necessary to modify the code of ~~ISSM~~ ISSM to implement the adapter, but future extensions may require such changes.

The ~~CUAS-preCICE~~ CUAS-preCICE adapter is an early prototype and does not yet follow most of the guidelines for ~~preCICE~~ preCICE adapters. Specific adaptations had to be made to ~~CUAS~~ CUAS to support the coupling with ~~ISSM~~ISSM. These can be generalized to open the adapter for different use cases. In addition, the adapter needs to be cleanly integrated into the code, as ~~CUAS-MPI~~ CUAS-MPI itself aims for a high degree of software quality.

We have demonstrated the stability and functionality of the coupled system in Sect. 3.1. Within both 1-way and 2-way coupling, the fields for N, v_b, T_e and H are consistent, indicating that the hydrological system is well set up. Our results reveal that the differences between the physical fields in 1- and 2-way coupling are significantly larger with high seasonal forcing. The larger the runoff, the more important ~~is a multi-physics approach~~ a multiphysics approach is. The more realistic feedback

is found by using 2-way coupling, as the two systems adapt to a joint state with reasonable physical fields in both systems. The time series (Fig. 6) exemplifies that the winter state in the runoff forced case has a higher $\overline{\log(T_e)}$ in winter than without seasonal runoff, which is reasonable. The lower $\overline{\log(T_e)}$ in the 2-way coupling corresponds to lower $\bar{N}$ in the high runoff forcing and vice versa, as N also influences the evolution of T_e. To summarize, the behavior of the ice and hydrology systems are reasonable, the simulated feedback is expected, but the drastic difference in 2-way coupling was not expected to this extent. As this paper focuses on the technical aspects of the coupling, we have not quantified the numerical accuracy of the coupled system nor fully demonstrated its ability to represent real-world cases. We have also not fully explored all ~~preCICE~~ preCICE features. In particular, informed choices need to be made regarding the optimal coupling scheme and the data mapping method.

Our performance experiments in Sect. 3.2 show that ~~preCICE~~ preCICE coupling does not negatively affect scaling during the simulation. Data mapping has negligible computational overhead, enabling coupling windows at least as short as the ~~ISSM~~ ISSM time step. ~~preCICE~~ preCICE time interpolation can be used in the future to improve temporal resolution if necessary, as shortening the ~~ISSM~~ ISSM time step would be expensive. Adaptive coupling windows would also be an option, but are not currently supported by ~~preCICE~~preCICE.

Serial coupling is around 5 % faster than parallel coupling up to 1024 processes. There is tentative evidence that parallel coupling widens the range of CPU counts that can be used efficiently. On the other hand, an imbalance in ~~scaling of the solvers limits~~ the solver scaling limits the scaling of the coupled system. Reducing the imbalance by redistributing CPUs does not significantly improve overall execution times because it involves reassigning CPUs from well-scaling ~~CUAS~~ CUAS to worse-scaling ~~ISSM~~ISSM. If there are many runs with the same number of CPUs and similar setups, it may be worth searching for the optimal distribution. Otherwise, an approximate solution is sufficient and probably uses fewer resources overall. It is also technically easier to allocate a distribution where every solver is assigned entire cluster nodes.

The cost of coupling and data mapping is ~~more significant~~ higher during initialization than during the actual simulation. Partitioning the coupling mesh and computing the mapping weights takes about the same amount of time as initializing the solvers themselves. The required time depends on the chosen mapping method. Linear cell interpolation, a second order method, is twice as expensive as first-order nearest neighbor interpolation. The partition-of-unity method shows promising performance for second-order (or higher) mapping, particularly the initialization times, but algorithmic improvements and special handling of discontinuous fields (e.g., specially adapted meshes) are required for it to be suited for our setup.

Other researchers have reported (sometimes significantly) faster initialization times for other couplers for comparatively sized setups, for example YAC (Hanke et al., 2016; Hanke and Redler, 2019) or C-CouplerLiu et al. (2023). As noted, we have not performed analysis of the initialization process internal to preCICE. Based on the profiles included in the supplement to this paper Abele et al. (2026) we believe that partitioning of the meshes, which in preCICE currently requires disk IO, is a contributor and could also be responsible for the slower initialization time of LCI over NN mapping.

The performance results give future users a basis for how to run the coupling efficiently. The relative solver and coupling execution times depend on too many factors (meshes, parameters, tolerances, etc.) to cover here. But estimates can be used to translate our results to other setups. Unlike the computation during simulation, initialization takes more time with added

processes. Therefore, the length of the simulation, and with it the balance of initialization and simulation time, ~~need~~ needs to be considered when choosing ~~which~~ how to allocate resources.

~~preCICE~~ preCICE has so far not been widely used in the ~~earth system modeling~~ Earth System Modeling community. While few (if any) ready-to-use adapters relevant to ~~earth system modeling~~ Earth System Modeling exist at the moment, developing such adapters is a current opportunity. Besides ESM-specific codes, models in frameworks like OpenFOAM, Elmer, or FEniCS/FEniCSx, for which ~~preCICE~~ preCICE adapters already exist, can be coupled with minimal effort. This makes these frameworks a good choice for the development of new models. For example, the ice sheet code Elmer/Ice could easily be coupled to ~~CUAS-MPI~~ CUAS-MPI using the adapters presented in this work. As mentioned in the introduction, Elmer/Ice already includes a different hydrology model, but being able to compare different approaches is highly valuable, as demonstrated by the various model intercomparison projects.

Without implementing comparable adapters for the same models, it is not possible to make a strong determination whether to prefer ~~preCICE~~ preCICE over a coupling library like YAC (Hanke et al., 2016) or OASIS3-MCT (Craig et al., 2017) that are specialized on ~~earth system models. We believe preCICE is at least on par regarding the basic functionality~~Earth System Models. We found that preCICE works very well in our setup. The software is mature. Basic adapters can be developed quickly, but of course a generic adapter for a large model like ~~ISSM~~ ISSM still requires significant effort to build and maintain. The adapters that we presented here, as well as the other existing adapters~~show that preCICE~~ , show that preCICE is compatible with ~~any solver architecture. The regridding benchmark by Hocks and Uekermann (2026) already demonstrated that numerical performance is equivalent. The results in Sect. 3.2 are in line with those reported for other libraries (Craig et al., 2017; Hanke et al., 2016), but a full benchmark – maybe an extension to the aforementioned regridding benchmark – with identical meshes would be necessary to get an accurate picture. The features of preCICE~~ various solver architectures. The features of preCICE (mapping methods, cartesian coordinates) are ~~well suited for the use casediscussed here. However, we have identified several missing features (spherical coordinate systems, masking, specialized mapping methods) that may be~~ well-suited for our use case, and the library provides potentially beneficial features such as time interpolation (Rodenberg and Uekermann, 2025) that can be enabled in the future with extensions to the ISSM and CUAS adapters. The absence of features provided by ESM-specific couplers did not impede our implementation, but they remain highly relevant for other ESM applications. Further development is probably needed to satisfy the requirements of the community. ~~The main advantage of preCICE due to its generic nature is~~ Features that are required or at least desirable include spherical coordinate systems, specialized conservative mapping methods, masking, temporal accumulation such as in OASIS3-MCT (Craig et al., 2017), loading of mapping weight files, support for calendars, and others. Above, we also discussed issues in initialization performance that require further investigation and optimization. A comprehensive comparison of the numerical and computational performance of the mapping methods using identical meshes is also necessary. We think, this effort is warranted due to the potentially much larger community ~~, collaborating~~ that multidisciplinary cooperation in the development of ~~adapters and the coupling library itself~~coupling libraries and adapters brings.

5 Conclusions

In this paper, we presented the software for coupling the ice sheet model ~~ISSM~~ ISSM to the subglacial hydrology model ~~CUAS-MPI~~CUAS-MPI. The main work has been to develop the adapters for the models for the coupling library ~~preCICE. The ISSM~~ preCICE. The ISSM adapter is generic and supports other use cases such as ice-ocean coupling, but adaptations will probably be necessary in some cases. The ~~CUAS-MPI~~ CUAS-MPI adapter is still a prototype and specific to coupling with ~~ISSM~~ISSM. Future development will focus on generalizing the adapter and better integrating it into the ~~CUAS-MPI~~ CUAS-MPI code.

The coupling is easy to use, adaptable, and extensible due to the generic coupling library. We have demonstrated its functionality in a synthetic setup to verify its correctness and stability. We have also analyzed different aspects of the system's performance, including initialization times, scaling, and mapping methods. The system scales well with the number of processes, and the overhead for coupling is low. These experiments can inform the efficient use of the software in the future. Comparatively slow initialization performance is a concern that should be addressed in further development.

We were able to at least qualitatively compare ~~preCICE~~ preCICE to libraries specialized on ~~earth system modeling~~Earth System Modeling. We found ~~preCICE~~ preCICE to be competitive in ~~all aspects , at least for the current use case, but closer analysis will be required to give a definitive answer. We identified~~ most aspects for our use case. However, in addition to the aforementioned performance issues, we have also identified some missing features that are required by other ESM applications. These are all possible future improvements for ~~preCICE~~ preCICE to better serve this community. ~~We also provided arguments that either approach is superior in the long run to integrating different models into the same monolithic code.~~

The new coupling will facilitate studies of the interaction between continental ice sheets and the hydrology systems underneath. We will also use the generic ~~ISSM-preCICE~~ ISSM-preCICE adapter in other setups. For example, we are developing a new solver for capturing the ice sheet calving fronts that can be coupled with ~~ISSM~~ ISSM to improve upon its existing moving front core. The use of ~~preCICE to integrate ISSM~~ preCICE to integrate ISSM into a global ~~earth system model~~ Earth System Model will be evaluated. Finally, the adapters can be extended to lift some of the limitations described in this paper and open even more use cases.

We hope that the software we developed enables researchers to implement and test new ice sheet model capabilities more quickly. In general, researchers should consider ~~preCICE~~ preCICE coupling when developing new models or extending existing ones.

Code and data availability. The current version of the ISSM-preCICE adapter is available at https://git.rwth-aachen.de/terrabyte-dnn2sim/issm-precice. Version 0.4.0 of the ISSM-preCICE adapter used in this paper is available at https://doi.org/10.5281/zenodo.18846020 (Abele and Humbert, 2026). The current version of CUAS-MPI is available at https://github.com/tudasc/CUAS-MPI. Version 0.1 of CUAS-MPI with added preCICE adapter used in this paper is available at https://doi.org/10.5281/zenodo.18846076 (Fischler et al., 2026). Input data, scripts to run the experiments and produce the plots for all the simulations presented in this paper, as well as results of performance measurements, are available at https://doi.org/10.5281/zenodo.18846105 (Abele et al., 2026)

Author contributions. DA developed the ISSM-preCICE adapter. YF and TK developed CUAS-MPI and the CUAS-preCICE adapter with contributions by DA. TK and DA ran the experiments to test functionality. DA ran the experiments to measure performance. AH supervised the project. CB supervised YF, HJB and AB supervised DA. MM provided support in the use of ISSM. BU and GC provided support in the use of preCICE. DA prepared the manuscript with significant contributions by TK, AH, BU, GC, and MM. All authors commented on and approved all parts of the manuscript.

Competing interests. The authors declare that they have no conflict of interest.

Acknowledgements. Part of this work was funded by HELMHOLTZ IMAGING, a platform of the Helmholtz Information & Data Science Incubator [grant number: ZT-I-PF-4-026].

We further thankfully acknowledge funding by the Deutsche Forschungsgemeinschaft (DFG, German Research Foundation) under Germany's Excellence Strategy EXC 2075 – 390740016 and under project number 528693298, and the support by the Stuttgart Center for Simulation Science (SimTech).

The authors gratefully acknowledge the computing time provided to them on the high-performance computer Lichtenberg 2 at the NHR Center NHR4CES at TU Darmstadt under grant p0020118. NHR4CES is funded by the Federal Ministry of Research, Technology and Space, and the state governments participating on the basis of the resolutions of the GWK for national high performance computing at universities.

We thank the reviewers Moritz Hanke and Basile de Fleurian for their great effort. This manuscript and our work was significantly improved by their in-depth comments.

References

Abele, D. and Humbert, A.: ISSM-preCICE adapter, https://doi.org/10.5281/zenodo.18846020, Zenodo [code], 2026.

Abele, D., Kleiner, T., Fischler, Y., and Humbert, A.: Coupling ISSM and CUAS-MPI: example cases, https://doi.org/10.5281/zenodo.18846020, Zenodo [data set], 2026.

Beyer, S., Kleiner, T., Aizinger, V., Rückamp, M., and Humbert, A.: A confined–unconfined aquifer model for subglacial hydrology and its application to the Northeast Greenland Ice Stream, The Cryosphere, 12, 3931–3947, https://doi.org/10.5194/tc-12-3931-2018, 2018.

Chourdakis, G., Davis, K., Rodenberg, B., Schulte, M., Simonis, F., Uekermann, B., Abrams, G., Bungartz, H., Cheung Yau, L., Desai, I., Eder, K., Hertrich, R., Lindner, F., Rusch, A., Sashko, D., Schneider, D., Totounferoush, A., Volland, D., Vollmer, P., and Koseomur, O.: preCICE v2: A sustainable and user-friendly coupling library [version 2; peer review: 2 approved], Open Research Europe, 2, https://doi.org/10.12688/openreseurope.14445.2, 2022.

Chourdakis, G., Schneider, D., and Uekermann, B.: OpenFOAM-preCICE: Coupling OpenFOAM with external solvers for multi-physics simulations, OpenFOAM® Journal, 3, 1–25, https://doi.org/10.51560/ofj.v3.88, 2023.

Craig, A., Valcke, S., and Coquart, L.: Development and performance of a new version of the OASIS coupler, OASIS3-MCT_3.0, Geoscientific Model Development, 10, 3297–3308, https://doi.org/10.5194/gmd-10-3297-2017, 2017.

de Fleurian, B., Morlighem, M., Seroussi, H., Rignot, E., van den Broeke, M. R., Kuipers Munneke, P., Mouginot, J., Smeets, P. C. J. P., and Tedstone, A. J.: A modeling study of the effect of runoff variability on the effective pressure beneath Russell Glacier, West Greenland, Journal of Geophysical Research: Earth Surface, 121, 1834–1848, https://doi.org/https://doi.org/10.1002/2016JF003842, 2016.

de Fleurian, B., Davy, R., and Langebroek, P. M.: Impact of runoff temporal distribution on ice dynamics, The Cryosphere, 16, 2265–2283, https://doi.org/10.5194/tc-16-2265-2022, 2022.

Desai, I., Scheurer, E., Bringedal, C., and Uekermann, B.: Micro Manager: a Python package for adaptive and flexible two-scale coupling, Journal of Open Source Software, 8, 5842, https://doi.org/10.21105/joss.05842, 2023.

ESMF Core Team: esmf-org/esmf: ESMF 8.9.1, https://doi.org/10.5281/zenodo.18167596, 2026.

Fischler, Y., Rückamp, M., Bischof, C., Aizinger, V., Morlighem, M., and Humbert, A.: A scalability study of the Ice-sheet and Sea-level System Model (ISSM, version 4.18), Geoscientific Model Development, 15, 3753–3771, https://doi.org/10.5194/gmd-15-3753-2022, 2022.

Fischler, Y., Kleiner, T., Bischof, C., Schmiedel, J., Sayag, R., Emunds, R., Oestreich, L. F., and Humbert, A.: A parallel implementation of the confined–unconfined aquifer system model for subglacial hydrology: design, verification, and performance analysis (CUAS-MPI v0.1.0), Geoscientific Model Development, 16, 5305–5322, https://doi.org/10.5194/gmd-16-5305-2023, 2023.

Fischler, Y., Kleiner, T., Abele, D., and Humbert, A.: CUAS-MPI with adapter for the preCICE coupling library, https://doi.org/10.5281/zenodo.18846076, Zenodo [code], 2026.

Gagliardini, O., Zwinger, T., Gillet-Chaulet, F., Durand, G., Favier, L., de Fleurian, B., Greve, R., Malinen, M., Martín, C., Råback, P., Ruokolainen, J., Sacchettini, M., Schäfer, M., Seddik, H., and Thies, J.: Capabilities and performance of Elmer/Ice, a new-generation ice sheet model, Geoscientific Model Development, 6, 1299–1318, https://doi.org/10.5194/gmd-6-1299-2013, 2013.

Hanke, M. and Redler, R.: New features with YAC 1.5.0, Reports on ICON, 3, https://doi.org/10.5676/DWD_pub/nwv/icon_003, 2019.

Hanke, M., Redler, R., Holfeld, T., and Yastremsky, M.: YAC 1.2.0: new aspects for coupling software in Earth system modelling, Geoscientific Model Development, 9, 2755–2769, https://doi.org/10.5194/gmd-9-2755-2016, 2016.

Hocks, A. and Uekermann, B.: Evaluation of preCICE (version 3.3.0) in an Earth System Model Regridding Benchmark, EGUsphere, 2026, 1–19, https://doi.org/10.5194/egusphere-2025-5618, 2026.

Huang, Q., Abdelmoula, A., Chourdakis, G., Rauleder, J., and Uekermann, B.: CFD/CSD coupling for an isolated rotor using preCICE, 14th World Congress of Computational Mechanics and ECCOMAS Congress, https://doi.org/0.23967/wccm-eccomas.2020.081, 2021.

Ing, R. N., Nienow, P. W., Sole, A. J., Tedstone, A. J., and Mankoff, K. D.: Minimal Impact of Late-Season Melt Events on Greenland Ice Sheet Annual Motion, Geophysical Research Letters, 51, e2023GL106 520, https://doi.org/https://doi.org/10.1029/2023GL106520, e2023GL106520 2023GL106520, 2024.

Jordan, J. R.: Calving Model Intercomparison (CalvingMIP) wiki, https://github.com/JRowanJordan/CalvingMIP/wiki, [Accessed 2025-02-26], 2024.

Keyes, D. E., McInnes, L. C., Woodward, C., Gropp, W., Myra, E., Pernice, M., Bell, J., Brown, J., Clo, A., Connors, J., et al.: Multiphysics simulations: Challenges and opportunities, The International Journal of High Performance Computing Applications, 27, 4–83, 2013.

Khrulev, C., Aschwanden, A., Bueler, E., Brown, J., Maxwell, D., Albrecht, T., Reese, R., Mengel, M., Martin, M., Winkelmann, R., Zeitz, M., Levermann, A., Feldmann, J., Garbe, J., Haseloff, M., Seguinot, J., Hinck, S., Kleiner, T., Fischer, E., Damsgaard, A., Lingle, C., van Pelt, W., Ziemen, F., Shemonski, N., Mankoff, K., Kennedy, J., Blum, K., Habermann, M., DellaGiustina, D., Hock, R., Kreuzer, M., Degregori, E., and Schoell, S.: Parallel Ice Sheet Model (PISM), https://doi.org/10.5281/zenodo.14991122, Zenodo [code], 2025.

Larour, E., Seroussi, H., Morlighem, M., and Rignot, E.: Continental scale, high order, high spatial resolution, ice sheet modeling using the Ice Sheet System Model (ISSM), Journal of Geophysical Research: Earth Surface, 117, https://doi.org/10.1029/2011JF002140, 2012.

Liu, L., Sun, C., Yu, X., Yu, H., Jiang, Q., Li, X., Li, R., Wang, B., Shen, X., and Yang, G.: C-Coupler3.0: an integrated coupler infrastructure for Earth system modelling, Geoscientific Model Development, 16, 2833–2850, https://doi.org/10.5194/gmd-16-2833-2023, 2023.

Martin, B. G.: Robust and Efficient Barycentric Cell-Interpolation for Volumetric Coupling with preCICE, Master's thesis, Technical University of Munich, 2022.

Mehl, M., Uekermann, B., Bijl, H., Blom, D., Gatzhammer, B., and van Zuijlen, A.: Parallel coupling numerics for partitioned fluid–structure interaction simulations, Computers & Mathematics with Applications, 71, 869–891, https://doi.org/10.1016/j.camwa.2015.12.025, 2016.

Noël, B., van de Berg, W. J., Lhermitte, S., and van den Broeke, M. R.: Rapid ablation zone expansion amplifies north Greenland mass loss, Science Advances, 5, https://doi.org/10.1126/sciadv.aaw0123, 2019.

Rodenberg, B. and Uekermann, B.: A waveform iteration implementation for black-box multi-rate higher-order coupling, https://doi.org/10.48550/arXiv.2511.07616, 2025.

Rodenberg, B., Desai, I., Hertrich, R., Jaust, A., and Uekermann, B.: FEniCS–preCICE: Coupling FEniCS to other simulation software, SoftwareX, 16, 100 807, https://doi.org/10.1016/j.softx.2021.100807, 2021.

Sasgen, I., Wouters, B., Gardner, A. S., King, M. D., Tedesco, M., Landerer, F. W., Dahle, C., Save, H., and Fettweis, X.: Return to rapid ice loss in Greenland and record loss in 2019 detected by the GRACE-FO satellites, Communications Earth & Environment, 1, https://doi.org/10.1038/s43247-020-0010-1, 2020.

Schneider, D. and Uekermann, B.: Efficient Partition-of-Unity Radial-Basis-Function Interpolation for Coupled Problems, SIAM Journal on Scientific Computing, 47, B558–B582, https://doi.org/10.1137/24M1663843, 2025.

Sommers, A., Rajaram, H., and Morlighem, M.: SHAKTI: Subglacial Hydrology and Kinetic, Transient Interactions v1.0, Geoscientific Model Development, 11, 2955–2974, https://doi.org/10.5194/gmd-11-2955-2018, 2018.

Tedesco, M. and Fettweis, X.: Unprecedented atmospheric conditions (1948 –2019) drive the 2019 exceptional melting season over the Greenland ice sheet, The Cryosphere, 14, 1209–1223, https://doi.org/10.5194/tc-14-1209-2020, 2020.

Teutsch, G. and Sauter, M.: Groundwater modeling in karst terranes: Scale effects, data acquisition and field validation, in: Proceedings of the Third Conference on Hydrogeology, Ecology, Monitoring and Management of Ground Water in Karst Terranes, Nashville, Tennessee, pp. 17–35, National Ground Water Association, Dublin, Ohio, 1991.

Totounferoush, A., Simonis, F., Uekermann, B., and Schulte, M.: Efficient and Scalable Initialization of Partitioned Coupled Simulations with preCICE, Algorithms, 14, https://doi.org/10.3390/a14060166, 2021.

Uekermann, B., Bungartz, H.-J., Cheung Yau, L., Chourdakis, G., and Rusch, A.: Official preCICE adapters for standard open-source solvers, pp. 210 – 213, GACM Colloquium on Computational Mechanics for Young Scientists from Academia and Industry, https://doi.org/10.18419/opus-9334, 2017.

Werder, M. A., Hewitt, I. J., Schoof, C. G., and Flowers, G. E.: Modeling channelized and distributed subglacial drainage in two dimensions, Journal of Geophysical Research: Earth Surface, 118, 2140–2158, https://doi.org/https://doi.org/10.1002/jgrf.20146, 2013.

Wolovick, M., Humbert, A., Kleiner, T., and Rückamp, M.: Regularization and L-curves in ice sheet inverse models: a case study in the Filchner–Ronne catchment, The Cryosphere, 17, 5027–5060, 2023.